GRAPHENE OXIDE AS A DRUG CARRIER FOR DELIVERY OF ZOLEDRONIC ACID IN SECONDARY BONE CANCER TREATMENT

by

SEPIDEH TAVAKOLI

B.S., Mechanical Engineering, University of Tehran, 2015

Submitted to the Institute of Biomedical Engineering

in partial fulfillment of the requirements

for the degree of

Master of Science

in

Biomedical Engineering

Boğaziçi University

2018

GRAPHENE OXIDE AS A DRUG CARRIER FOR DELIVERY OF ZOLEDRONIC ACID IN SECONDARY BONE CANCER TREATMENT

APPROVED BY:

Assist. Prof. Dr. Duygu Ege   . . . .
(Thesis Advisor)

Assoc. Prof. Dr. Bora Garipcan   . . . .

Assist. Prof. Dr. Osman Bulut   . . . .

DATE OF APPROVAL: 11 July 2018

ACKNOWLEDGMENTS

ACADEMIC ETHICS AND INTEGRITY STATEMENT

I, Sepideh Tavakoli, hereby certify that I am aware of the Academic Ethics and Integrity Policy issued by the Council of Higher Education (YÖK) and I fully acknowledge all the consequences due to its violation by plagiarism or any other way.

Name :   Signature:

_____   _____

Date:

_____

ABSTRACT

GRAPHENE OXIDE AS A DRUG CARRIER FOR DELIVERY OF ZOLEDRONIC ACID IN SECONDARY BONE CANCER TREATMENT

In this study, Zoledronic acid (ZOL), a type of nitrogen containing bisphosphonate, was loaded on graphene oxide (GO) particles to increase the particle size of the drug-nano-carrier complex which reduces drug filtration by the kidney and consequently, increases drug circulation time and its tumor uptake. The conjugation between ZOL and GO occurs via $\pi - \pi$ stacking and hydrogen bonding interactions, and therefore, the drug may be gradually released from GO in physiological conditions which eliminates the need to apply high doses of the drug. Loading and release profile of ZOL on GO particles was investigated by using UV-Vis spectroscopy. Samples with different concentrations of 0.025-1.25 mg/ml of ZOL were loaded on 0.2 mg/ml GO. UV analysis showed that the maximum loading happens at ZOL to GO ratio of 1:0.2. This loading was obtained when 1 mg/ml of ZOL was initially loaded on 0.2 mg/ml of GO nanoparticles. The drug and drug carrier complexes were characterized using Fourier-Transform Infrared Spectroscopy (FTIR), Atomic Force Microscopy (AFM), and UV-vis spectroscopy. Cell culture studies were carried out with MCF-7 breast cancer cells and mesenchymal stem cells (MSCs) for three dosages of ZOL, ZOL conjugated with GO (ZOL-GO) and GO. Cell proliferation was investigated by Alamar blue assay and cell viability was evaluated by staining dead cells with propidium iodide (PI) and live cells with acridine orange (AO). Overall, the characterization results confirm loading of ZOL on GO nanoparticles and cell studies results show that GO conjugated ZOL complexes are promising to reduce MCF-7 breast cancer cells proliferation and viability.

Keywords: ZOL, GO, Drug Loading, MCF-7, MSC.

ÖZET

İKİNCİL KEMİK KANSERİ TEDAVİSİNDE ZOLEDRONİK ASİTİN GRAFEN OKSİT İLAÇ TAŞIYICISI İLE KULLANIMI.

Bu çalışmada, nitrojen bazlı bir bisfosfonat olan zoledronik asit (ZOL), grafen oksit (GO) kompleksi geliştirilmiştir. Bu sayede ilaç partikül boyutu arttırılarak böbrekteki ilaç filtrasyonu düşürülebilir ve ilaç sirkülasyon süresi ve tümör alımı arttırılabilir. ZOL ve GO arasındaki konjugasyon $\pi - \pi$ etkileşimleri ve hidrojen bağı ile kurulur ve fizyolojik ortamda ilaç zaman içerisinde salınır. Sonuç olarak yüksek dozda ilaç kullanmaya gerek kalmaması hedeflenmektedir. Bu amaca yönelik olarak öncelikle UV spektroskopisi ile ZOL'un GO üzerine yüklenme salınım profilleri incelendi. 0.025-1.25 mg/ml aralığında ZOL, 0.2 mg/ml GO üzerine yüklendi. UV analizi maksimum yüklemenin 1:0.2 oranında gerçekleştiğini gösterdi. Bu yükleme miktarı 1 mg/ml ZOL'un 0.2 mg/ml GO nanopartiküllerine ilave edilmesiyle elde edildi. İlaç ve ilaç taşıyıcı kompleksleri FTIR, AFM, UV spektroskopisi ile analiz edildi. Hücre kültürü çalışmaları MCF-7 meme kanseri ve mezenkimal kök (MSC) hücreleriyle üç farklı dozda ZOL, ZOL-GO ve GO için gerçekleştirildi. Hücre çoğalması Alamar blue analizi ile, hücre, ölü hücreler propidium iyodu ve canlı hücreler da ölü hücrelerin propidium iyodu (PI), canlı hücrelerin akridin turuncusu (AO) ile boyanmasıyla tespit edildi. Sonuç olarak, ZOL'un GO nanoparçacıklarının üzerine bağlandığı karakterizasyon çalışmaları ile belirlendi. Çoğalma ve canlılık ile ilgili hücre kültürü çalışmaları ise GO-ZOL kompleksinin MCF-7 meme kanseri hücrelerinin azalmasında etkili olduğunu gösterdi.

Anahtar Sözcükler: ZOL, GO, İlaç yükleme, MCF-7, MSC.

TABLE OF CONTENTS

LIST OF FIGURES

LIST OF TABLES

LIST OF SYMBOLS

℃	Degrees Centigrade
h	Hours
g	Grams
λ	Lambda
μM	Micro Molar
mM	Milli Molar
mg	Milli Grams
ml	Milli Liter
nm	Nano Meter
kDa	Kilo Daltons
μl	Micro Liter
cm	Centimeter

LIST OF ABBREVIATIONS

ZOL	Zoledronic Acid
GO	Graphene Oxide
NGO	Nano-Graphene Oxide
CO2	Carbon Dioxide
ATCC	American Type Culture Collection
dH_2O	Distilled water
PBS	Phosphate Buffer Solution
MCF-7	Michigan Cancer Foundation-7
ADR	Adriamycin
ZOL-GO	Zoledronic Acid conjugated to Graphene Oxide
ECM	Extra cellular Matrix
PTHrP	Parathyroid Hormone-related Peptide
IL-6	Interleukin-6
RANK L	Receptor Activator of Nuclear Factor-κB Ligand
IGF-1	Insulin-like Growth Factor-1
TGF-β	Transforming Growth Factor-β
PDGF	Platelet-Derived Growth Factor
ATP	Adenosine Triphosphate
$\gamma\delta$T cell	Gamma Delta T cell
MMP	Matrix Metalloproteinase
VEGF	Vascular Endothelial Growth Factor
PBPs	Penicillin Binding Protein
EPR	Enhanced Permeability and Retention
PC3	Human Prostate Cancer Cell Line 3
PEG	Polyethylene Glycol
PLGA	Poly(Lactic-Co-Glycolic Acid)
HCT-116	Human Colon Cancer Cell Line-116
CPT	Camptothecin

DOX	Doxorubicin
UV-vis	Ultraviolot-Visible
FTIR	Fourier-Transform Infrared Spectroscopy
AFM	Atomic Force Microscopy
MWCO	Molecular Weight Cut-Off
PBS	Phosphate Buffer Saline
FBS	Fetal Bovine Serum
PI	Propidium Iodide
AO	Acridine Orange
MDA-MB-231	Triple Negative Breast Cancer Cell Line
FA	Folic Acid
rGO	Reduced Graphene Oxide
MSCs	Mesenchymal Stem Cells

1. INTRODUCTION

1.1 Motivation

Secondary bone cancer is a malignant disease which decreases the patient's chance of survival significantly [1–3]. One of the most effective treatments for secondary bone cancer is chemotherapy [4]. As an example, bisphonsphonates are used for decades as a treatment for secondary bone cancer. Zoledronic acide (ZOL) is a type of bisphosphonate which is effective in reducing number of tumor cells and inhibits bone resorbtion [1]. Despite all the useful effects of ZOL, using free drug is not efficient due to several reasons. For example, kidney can easily filter its small molecules even before reaching to the site of the tumor [5]. As a result, higher doses of drug must be administered which means higher chances of occurrence of side effects. So finding an appropriate drug carrier for ZOL has recently became a challenging research area.

Graphene oxide (GO) is one atom thick layer of graphene which has been used as a drug carrier for many anti-cancer drugs. For instance, Yang et al. [6] used GO as a drug carrier for Doxorubicin (DOX). Zhang et al. [7] also used GO as a carrier for mixed anti-cancer drugs of Doxorubicin (DOX) and Camptothecin (CPT).

Since both GO nanoparticles and ZOL contain aromatic rings in their chemical structure, ZOL could conjugate with GO by non-covalent $\pi-\pi$ interactions. In addition to $\pi-\pi$ stacking, based on ZOL (Figure 2.4) and GO (Figure 2.6) structure, hydrogen bonding and hydrophobic interactions are also occur. Conjugation of ZOL on GO nanoparticle increases the size of the complex which reduces fast renal filteration and concequently increases the circulation time throughout the body [8]. Furthermore, slow release of ZOL from GO prevents harmful side effects which mostly result from the presence of high doses of drug in the body [6]. Moreover, as the size of the drug complex increases, the chance of crossing the blood-brain barrier decreases which avoids neurotoxicity effects [1].

The anti-cancer effect of ZOL on MCF-7 breast cancer cells are observed in many studies such as Torger et al. [9] and Jagdev et al. [10] works. Furthermore, Wu et al. [11] observed that treating MCF-7 with adriamycin (ADR) conjugated to GO shows lower relative cell viability than free ADR. So MCF-7 breast cancer cells might be a good candidate for investigating the anti-cancer effect of onjugation of ZOL and GO (ZOL-GO). Ebert et al. [12] investigated the effect of ZOL on mesenchymal stem cells (MSCs) and they observed that ZOL in vitro inhibits MSCs proliferation. So, treating MSCs with free ZOL and ZOL-GO and compare the results with previous study might be useful.

In this work, we prepared the conjugation of ZOL and GO. The conjugation between ZOL and GO was characterized by FTIR, AFM and UV-vis spectroscopy. Loading of ZOL on GO and release of it from ZOL-GO investigated by UV-vis spectroscopy. We treated MCF-7 cancer cells and MSCs with our experimental groups (ZOL, ZOL-GO and ZOL). This way, effect of conjugation of ZOL and GO would be investigated on MCF-7 and MSCs proliferation and cell viability.

1.2 Objectives

The aim of this study is to improve the effect of ZOL on tumor cells by using GO nanoparticles as a drug carrier.
The main objectives of this study are presented below:

- To Prepare the conjugation of GO and ZOL based on the $\pi - \pi$ interaction between aromatic rings in the chemical structure of GO and ZOL.

- To characterize the conjugation between GO and ZOL.

- To investigate the optimum amount of ZOL loading on the drug carrier GO.

- To investigate in vitro ZOL release from GO.

- To examine the effect of ZOL-GO complex treatment on MCF-7 breast cancer cells and compare the results with treatment with free ZOL.

- To examine the effect of ZOL-GO complex treatment on MSCs and compare the results with treatment with free ZOL.

1.3   Outline

This thesis is composed of five chapters. Chapter 1 is an introduction which contains motivation and objectives . Chapter 2 provides background information about secondary bone cancer, bisphosphonates and their mechanism of actions, the structure and applications of GO are also reviewed in this chapter. In Chapter 3, experimental procedures are explained and in Chapter 4 the results are presented. Finally, in Chapter 5 discussion, conclusion and suggestions for future works are given.

2. BACKGROUND

2.1   Secondary Bone Cancer

Bone metastasis is a secondary cancer which significantly reduces patient's chance of survival [1–3]. One of the reasons of bone metastasis is invasion of primary tumor cells to the bone. Figure 2.1 shows three different stages of metastatic cascade of tumor cells. Cancer cells escape from their tissue of origin after degrading the extra cellular matrix (ECM) and entering the blood circulation, then they enter the bone tissue [1]. Primary cancer types such as breast, prostate, lung, thyroid, renal, multiple myeloma and oral cancers have the potential to cause bone metastasis [13]. Nearly three quarters of the advanced breast and prostate cancer patients will experience metastasis in the form of secondary bone cancer and consequently end up with lower chance of survival [1].
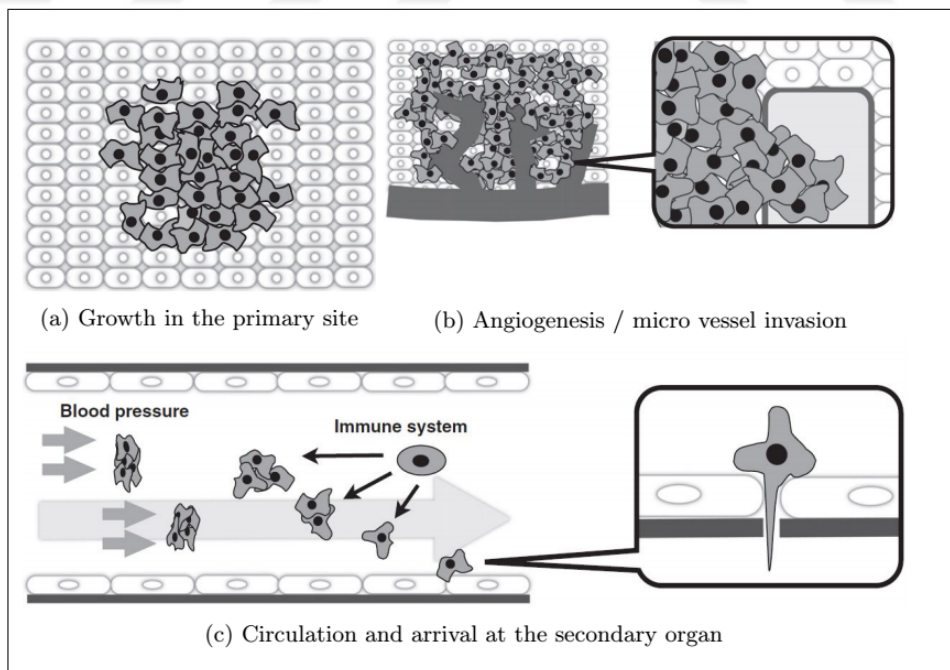

(a) Growth in the primary site   (b) Angiogenesis / micro vessel invasion

(c) Circulation and arrival at the secondary organ

Figure 2.1 Metastatic cascade of tumor cells [14].

2.1.1   Affinity of Cancer Cells to the Bone

Bone tissue is home to the cells such as osteoblasts and osteoclasts which are responsible for producing and dissolving of bone tissue, respectively. Bone cells such as osteoblasts and osteoclasts mutually interact with tumor cells which leads to a "vicious cycle" and further tumor development. Brifely, tumor cells release specific proteins which increases osteoclast activity and bone resorbtion which concequently increase releasing of growth factors which enhance tumor cell proliferation. This is known as the "vicious cycle". So, bone microenvironment provides a favorable place for tumor cells to survive and grow which increases the probability of metastasis [14, 15]. Many studies have shown that the metastasis in the bone not only effects the interaction between osteoblast and osteoclast but also other cell types; such as immune cells (T and B cells, macrophages and natural killer cells) and fibroblasts [13, 16, 17].

2.1.2   Cancer Cells in the Bone

Following the entrance of tumor cells to the bone microenvironment with the aid of proteolytic enzymes, cancer cells invade the bone marrow stroma and induce blood supply for their own. Based on the nature of the tumor, cancer cells can affect osteoblast or osteoclast activity [18]. In the bone microenvironment, tumor cells increase osteoclasts activity by releasing parathyroid hormone-related peptide (PTHrP), interleukin-6 (IL-6) and activating RANKL expression in osteoblast. This leads to an increase in bone resorption and consequently releasing growth factors such as insulin-like growth factor-1 (IGF-1), transforming growth factor-β(TGF-β) and platelet derived growth factor (PDGF). The release of these growth factors increase tumor cell proliferation [19]. This cycle is know as a "vicious cycle" which is shown in Figure 2.2.
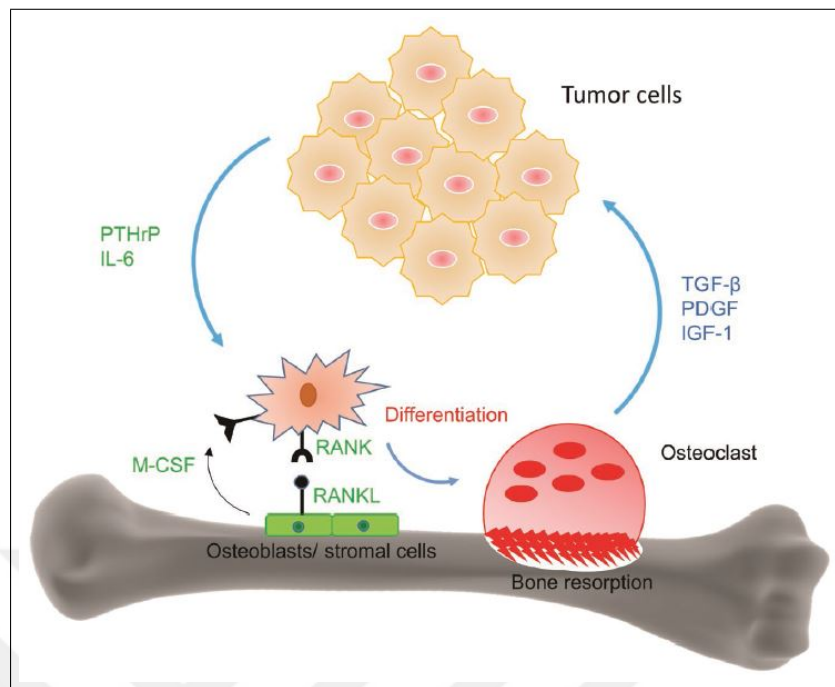
Figure 2.2 Vicious cycle of bone niche [1].

2.1.3   Secondary Bone Cancer Cures

There are many different types of cancer treatment. Surgery, radiotherapy and chemotherapy. Surgery is mostly effective when cancer is at its first stage. So in secondary bone cancer, surgery is rarely considered because cancer cells are not just in their primary region and they have metastasized. Radiotherapy is another method which involvs use of high energy radiation to kill cancer cells. In secondary bone cancer, radiotherapy is not highly recommended because cancer cells have already spread throughout the body. In chemotherapy an anti-cancer drug is used to circulate in blood throughout the body and reach the tumor. Therefore, chemotherapy is the most preferred form of therapy in secondary bone cancer [1].

There is a hypothesis that bone disease could be treated by inhibiting osteo-clasts activity, as it enhance bone integrity and decrease the tumor proliferation and survival [20]. Recently, many studies have been done on new therapeutic agents for bone metastasis treatment [1], among them, using bisphosphonates is one of the most attractive therapies. Studies confirm that bisphosphonates can prevent metastasis of

cancer at the early stages and also decrease bone absorption caused by metastasis [21, 22].

Bisphosphonates initially considered as osteoporotic drugs [23] and have been used as a clinical anti-resorption treatment for a long time. Bisphosphonates have been used for diseases such as secondary bone cancer, osteoporosis, Paget's disease and fibrous dysplasia [24].

2.2   Bisphosphonates

2.2.1   Structure and Types

Structure of bisphosphonate is similar to the structure of inorganic pyrophosphate's (P-O-P), but instead of oxygen, there is a carbon molecule at the center (P-C-P). Two additional side groups of R1 and R2 are different in each type of bisphosphonate [25].

We could classify bisphosphonates based on their generation and chemical structure. Structure of bisphosphonates might be either with nitrogen (amino- bisphosphonates) or without nitrogen (non-amino-bisphosphonates). Clodronate, tiludronate and etidronate are the examples of non-nitrogen containing bisphosphonates. Examples of the second generation of nitrogen-containing bisphosphonates are alendronate, pamidronate and ibandronate and third generation examples are zoledronate and risedronate [26]. Figure 2.3 shows the chemical structure of some clinically used bisphosphonates and Figure 2.4 shows zoledronic acid chemical structure.
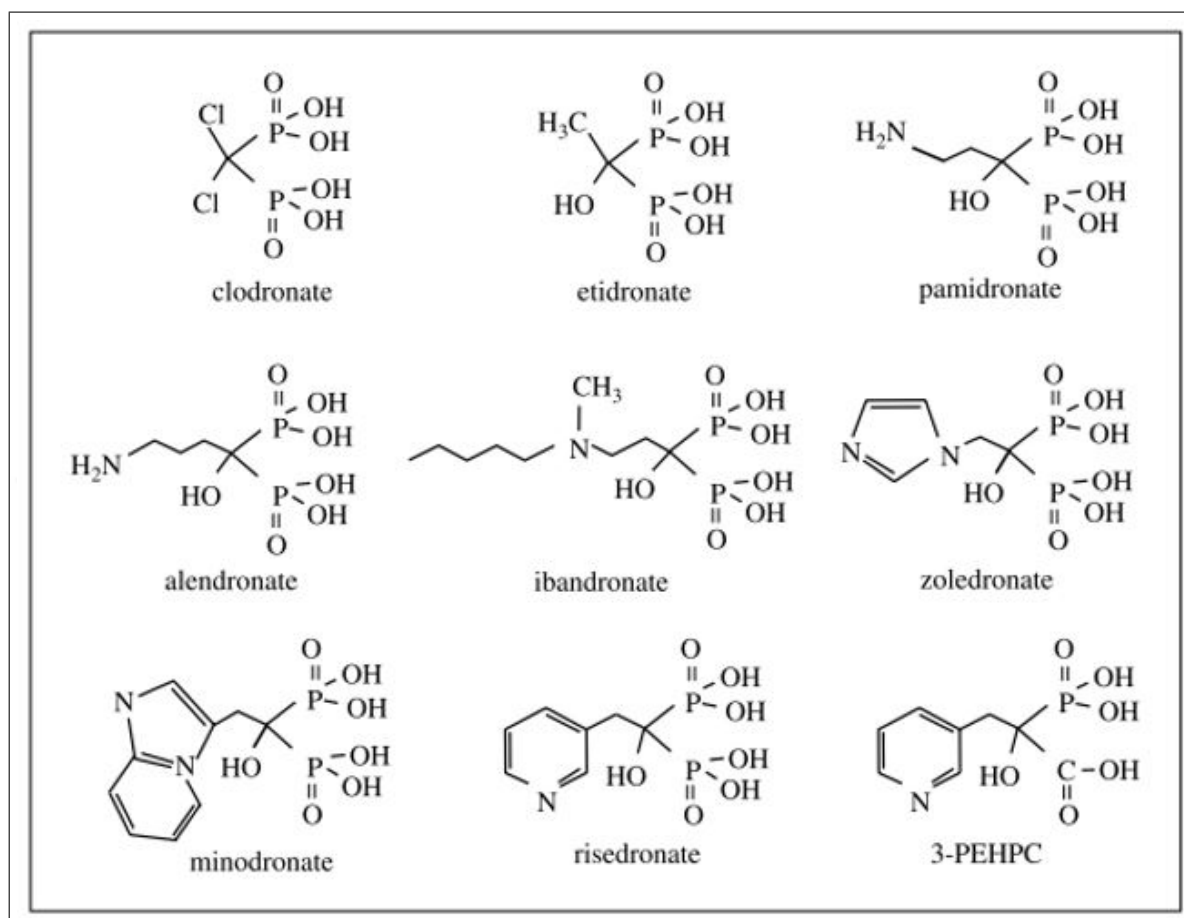
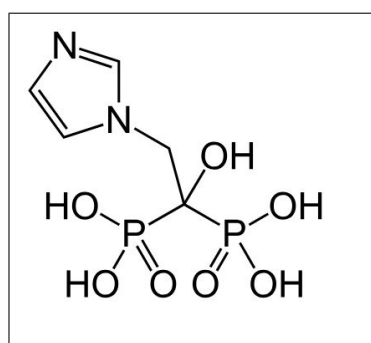**Figure 2.3** Structure and types of bisphosphonates [27].

Figure 2.4 Chemical Structure of Zoledronic Acid [28].

2.2.2 Bisphosphonates Affinity to Bone

Bisphosphonates have high affinity to bone minerals [29]. They bind to the bone minerals such as hydroxyapatite in the bone extracellular matrix. This selective attraction leads to lower systemic toxicity [30]. Bisphosphonate affinity to hydroxyapatite is higher than its affinity to other calcium-based minerals such as carbonate, pyrophosphate and oxalate [31]. As we observe increase in the exposure of hydroxyapatite in bone metastasis, the higher affinity of bisphosphonates to hydroxyapatite could be useful for targeting and accumulation of the drug to the aimed area [32]. ZOL is a third generation of nitrogen containing bisphosphonate which has more affinity to hydroxyapatite than all the other types of bisphosphonates. Henneman et al. [33] ranked bisphosphonates based on their binding affinity: zoledronate>alendronate>ibandronate>risedronate>etidronate>clodronate.

The affinity of bisphosphonates to hydroxyapatite depends on side groups of R1 and R2. Ion exchange and chemisorption process between inorganic phase of extracellular matrix and phosphonate group of bisphosphonates are responsible for accumulation of bisphosphonate in the bone tissue [34].

Two phosphonate groups of bisphosphonates cause chelation of calcium ions on the surface of hydroxyapatite which results in the formation of bidentate bond [35]. The affinity of the drug to bone mineral is enhanced if the R1 side group is substituted with hydroxyl group [36]. R2 group was expected to have only pharmacological effect, but in some studies we observed the higher affinity of bisphosphonates with nitrogen in their R2 group compared to the ones without nitrogen [25]. The difference between the affinity of nitrogen-free and nitrogen-containing bisphosphonates to the bone mineral comes from the difference between the zeta potential of hydroxyapatite surface. The reason is that mineral surface is more positively charged after bonding to nitrogen-containing R2. Therefore the binding to negatively charged phosphonate group of bisphosphonates is enhanced. Furthermore, amino group in amino-bisphosphonates form hydrogen bond with hydroxyapatite surface [36].

2.2.3   Mechanism of Action

There are two mechanisms of action of bisphosphonates on cancer cells, direct and indirect. In direct mechanism cancer cells undergo apoptosis. In many in vitro studies, anti-tumor effect of bisphosphonates have been shown to inhibit tumor cell growth and adhesion to the bone, inducing tumor cell apoptosis and reducing tumor cell invasion [37]. Indirect mechanism, on the other hand, is inhibiting excess bone resorption by killing osteoclasts. This action interferes with malicious cycle and reduces the tumor's growth factors which are released from osteoclasts or bone matrix while resorption happens [29]. The mechanism of action is different depending on the type of bisphosphonate. Generally, bisphosphonates have both anti-resorptive and anti-tumor mechanism of action [1]. Figure 2.5 summarizes the direct and indirect effect of nitrogen-containing bisphosphonates on cancer cells.

Anti-resorptive mechanism of action of bisphosphonates indirectly inhibits tumor growth. This mechanism is different between amino-bisphosphonates and non-amino- bisphosphonates. Non-amino-bisphosphonates induce osteoclast apoptosis by causing deficiency in functional adenosine triphosphate (ATP) [38]. Amino- bisphosphonates on the other hand inhibit protein prenylation and malevolent pathway which leads to osteoclast apoptosis [39].

Anti-tumor activity of bisphosphonates contains reduction of cell growth, adhesion, invasion and angiogenesis as well as an increase in immune activity which leads to tumor cell apoptosis. Bisphosphonates induce host immune responses in the malevolent pathway by activating $\gamma\delta$ T cells (Gamma Delta T cells) [40–42]. Bisphosphonates directly affect tumor cells by inducing tumor cell apoptosis and inhibiting tumor growth. This effect has been validated in a mouse model for multiple myeloma [29]. Bisphosphonates inhibit adhesion and invasion of tumor cells which are important factors for the start of metastasis. Tumor invasion is facilitated by Matrix Metalloproteinases (MMPs) [43]. Bisphosphonates like ZOL inhibit production of MMPs such as MMP-1 [44]. In addition, bisphosphonates inhibit proteolytic activity of some other MMP's like MMP-2 and MMP-9 which leads to decrease in tumor cell invasion [45]. Bisphos-

phonates suppress vascular endothelial growth factor (VEGF) which leads to inhibition of tumor angiogenesis. Bisphosphonates play an important role in reduction Of the tumor burden, because the development of tumor highly depends on angiogenesis [46]. In some studies, the direct effect of bisphosphonats on cancer cells was observed on breast cancer [47], melanoma [48], and cervical cancer [49].
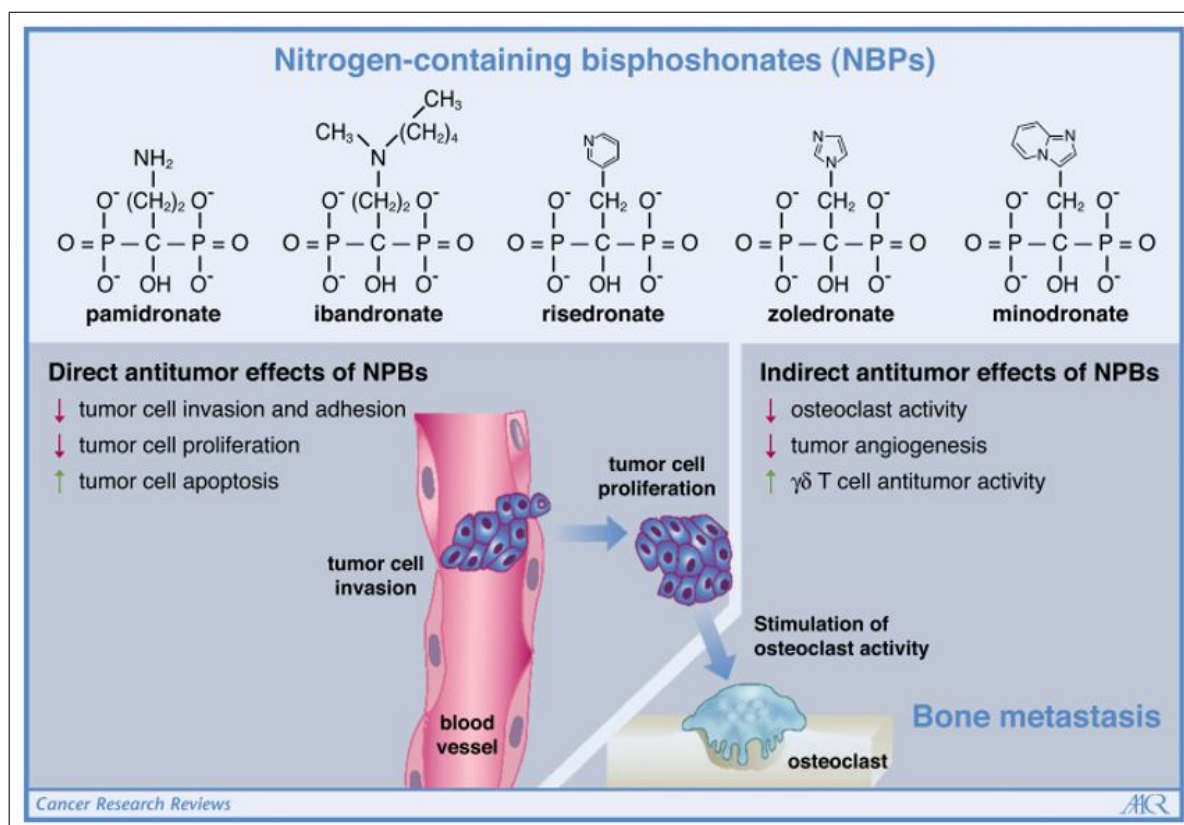
Figure 2.5 Nitrogen-containing bisphosphonates direct and indirect anti-tumor effect [37].

2.2.4 Side Effects and Difficulties of Using Bisphosphonates

Bioavailability in oral administration of bisphosphonates is about 3-7% which is very low [50, 51]. High doses of intravenous administration of bisphosphonate increase the bioavailability of the drug, however it significantly increases the chance of osteonecrosis of jaw [52–55], kidney complication [56, 57] and electrolyte abnormalities

[58]. In addition, some bisphosphonates such as ZOL are small molecules, so they are cleared by renal system in a short time. This might cause excretion of the drug even before reaching to the target [5].

2.2.5 Advantages and Techniques of Conjugation of Nanocarriers and Drug

Conjugation of nano-carriers to drugs such as nanoparticles shows many advantages. The abrupt increase of the drug dose in intravenously administered bisphosphonate treatment can be solved by conjugation of the bisphosphonate with a carrier. This would lead to gradual release of drug from drug carrier and this inhibits existence of high doses of drug in the body thus reduces the side effects [6]. In addition, using an appropriate drug carrier increases the volume of the drug, which prevents fast clearance of the drug by kidney. As a result, circulation time increases. Therefore, the drug would have more time to be near the tumor and have an effect on osteoclasts and cancer cells [8]. The increase of the size would also decrease the chance of crossing the blood-brain barrier and prevent neurotoxicity [1, 56, 59] .

There are many studies in which bisphosphonates have been conjugated to nano-carriers such as bisphosphonates-functionalized liposome or nanoparticle [1]. For example Marra et al. [57] encapsulated ZOL in liposomes targeting prostate cancer and multiple myeloma using PC3 and OPM2 tumor cell lines. Marra et al. [60] in another study produced ZOL-self assembled PEGylated nano-drug delivery vehicles for prostate cancer using PC3M-luc2 cells. Chaudhari et al. [61] loaded ZOL and docetaxel on PLGA nanoparticles conjugated by N,N' -Carbonyldiimidazole linker for bone tumor targeted drug delivery application.

2.3 Graphene Oxide

Graphene-based nanomaterial has potential in drug delivery field as a drug carrier based on the large surface area and drug loading capacity via $\pi - \pi$ stacking

and hydrophobic interaction. GO is one atom thick layer of graphite which consists of carboxylic acid, epoxide and hydroxyl group. Hydroxide and epoxide have no charge, but they could be responsible for hydrogen binding and polar interactions. Free surface π electrons of plates provide opportunity of loading drug by means of $\pi - \pi$ interaction [62]. Figure 2.6 compares the chemical structure of graphite and graphene oxide.

One of the earliest studies in the field of drug delivery was done by Lio et al. [62]. They loaded SN38 on PEG−functionalized nanoscale GO (NGO) sheets. NGO−PEG−SN38 showed high toxicity in HCT−116 cells and good water solubility. Wu et al. [11] used GO as a carrier for Adriamycin (ADR) and observed drug resistance reversal in MCF−7/ADR, high loading capacity and PH sensitive drug release. Zhang et al. [7] studied GO as a carrier for multiple drugs co−delivery for the first time. They used doxorubicin (DOX) and camptothecin (CPT) loaded on GO−sulfonic acid. They reported higher toxicity in MCF−7 cells than each drug, separately.
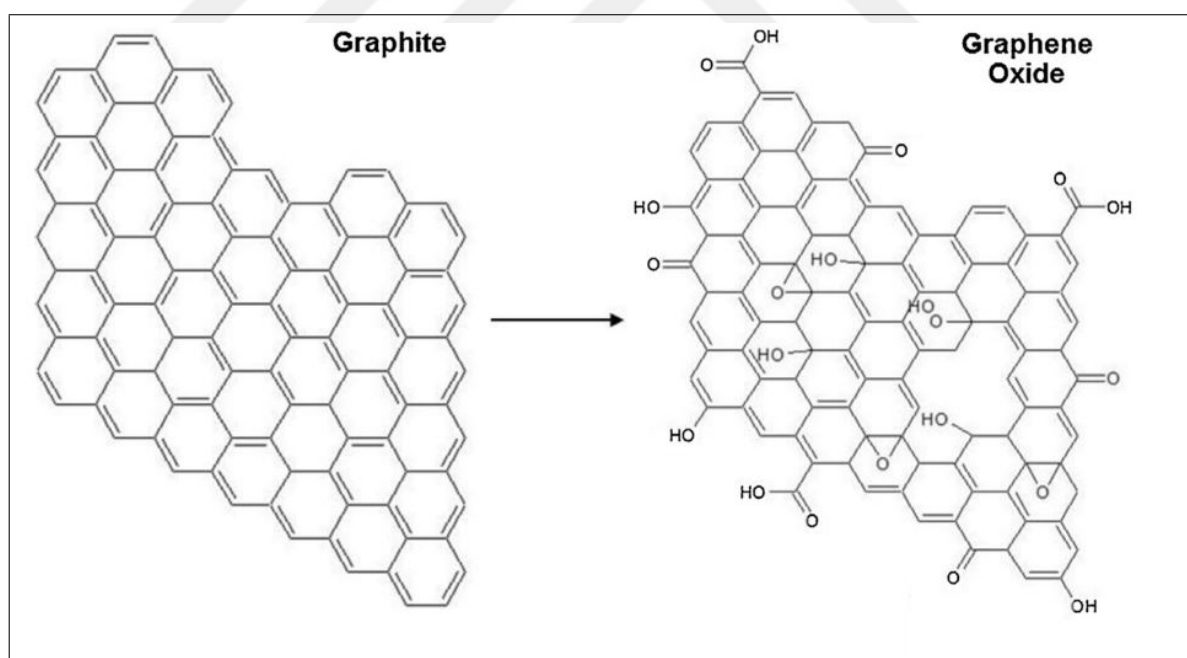

Figure 2.6 Graphite and Graphene Oxide structure [63].

3. MATERIALS AND METHODS

3.1 Conjugation of ZOL-GO

ZOL was loaded non-covalently on GO by simply mixing them together in ultra pure water. First, all the solutions were sonicated for 15 minutes, then stirred by magnetic stirrer at room temperature in the dark overnight [6].

3.2 UV-vis Spectroscopy

ZOL (1.25 mg/ml), GO (0.25 mg/ml) and ZOL-GO (1.25 mg/ml ZOL and 0.25 mg/ml GO) were prepared in ultra pure water. Then, samples were characterized by UV-vis spectrophotometer (Nanodrop 2000c Spectrophotometer, Thermo Scientific, USA). The wavelengths of 209 nm and 230 nm was considered as characteristic peaks of ZOL and GO, respectively.

3.3 Fourier Transform Infrared Spectroscopy (FTIR)

GO (0.25 mg/ml) and ZOL-GO (1.25 mg/ml ZOL and 0.25 mg/ml GO) were prepared in ultra pure water. The samples were washed with distilled water (dH_2O) several times to get rid of free drugs and dried by using filtration paper. To investigate the chemical composition of ZOL-GO, Thermo Scientific iS10 FTIR, single reflection diamond ATR was used. The FTIR spectra were recorded in the range of 4000 to 650 cm^{-1}. The FTIR analysis was performed at Koç University Surface Science and Technology Center (KUYTAM).

3.4   Atomic Force Microscopy (AFM)

ZOL (1.25 mg/ml), GO (0.25 mg/ml) and ZOL-GO (1.25 mg/ml ZOL and 0.25 mg/ml GO) were prepared in ultra pure water. Similar to previous section, the samples were washed with dH_2O several times and dried by using filtration paper. The morphology of GO before and after loading of ZOL was characterized by using Bruker Dimension Icon AFM in tapping mode at Koç University Surface Science and Technology Center (KUYTAM). The AFM images were analyzed by Nanoscope Analysis v150 processing software.

3.5   Drug Loading

The following steps were conducted to obtain the optimum drug loading. First, samples with the same concentration of GO (0.2 mg/ml) and different concentration of ZOL (0 to 1.25 mg/ml) were sonicated for 15 minutes and then stirred by a magnetic stirrer at room temperature in the dark overnight. Each sample was transferred with a needle in a 2-kDa Slide-A-Lyzer dialysis cassette (2K MWCO, 0.5 mL, Thermo Scientific) and dialysed against 10 ml distilled water which was constantly stirring by magnetic stirrer. After 24 hours, samples were taken out from distilled water and measured by UV-Spectrophotometer at wavelength of 209 nm. Calibration curve for ZOL at the wavelength of 209 nm is given in Appendix A. The amount of ZOL loaded on GO was calculated using Eq. 3.1.

$$Drug\ Loading\ Capacity\% = \frac{W_{administered\ ZOL} - W_{outer\ ZOL}}{W_{GO}} \times 100 \qquad (3.1)$$

where $W_{administered\ ZOL}$ is the weight of initial drug added to the solution, $W_{outer\ ZOL}$ is the weight of the free drug which is not loaded and exits the dialysis chamber and W_{GO} is the weight of GO added to the solution.

3.6   Drug Release

The optimum proportion of drug and drug carrier (1 mg/ml ZOL and 0.2 mg/ml GO), obtained from the drug loading part, was used to observe the drug release profile, for in vitro drug release. Aqueous solution of ZOL and GO with the concentration of 1 mg/ml and 0.2 mg/ml respectively was sonicated for 15 minutes and stirred at room temperature in the dark overnight. The next day, the solution was purred in a 2-kDa dialysis cassette and dialysis against 15 ml phosphate-buffered saline (PBS) at 37 ± 0.2 °C stirring constantly by magnetic stirrer. Each time, small sample of PBS was taken out and measured by UV-Spectrophotometer.

3.7   Cell Studies

MCF−7 human breast cancer cells (ATCC) were kindly provided by Assoc. Prof. Dr. Bora Garipcan (Boğaziçi University, Istanbul, Turkey) and they were used to investigate anti-tumor effect. MCF-7 cells were maintained in Dulbecco's Modified Eagle's Medium/Nutrient Mixture F−12 Ham (Sterile-filtered) supplemented with 10% fetal bovine serum (FBS, Gibco) and 1% Penicillin-Streptomycin (sterile-filtered, BioReagent, Sigma). The cells were seeded in a T−75 cell culture flask and incubated at 37 °C in a fully humidified incubator with 5% CO_2. When the cells covered almost 80 percent of the flask, the cells were counted and seeded in a 96 well plate (5000 cells in each well) with 100 μL medium in each well. The 96 well plate was incubated overnight to allow the cells to adhere to the plate. The next day, cells were treated for 72 hours with experimental groups. In table 3.1, experimental groups are identifies with check mark. 6 samples of each experimental group where studies.

Bone marrow mesenchymal stem cells (MSCs, ATCC) were also used to investigate the effect of our experimental groups. Cell study of MSCs protocol and experimental group were the same as what mentioned above. The only difference was using Mesenchymal Stem Cell Basal Medium (ATCC) for MSCs instead of DMEM/F12.

Table 3.1
Experimental groups for cell study.

ZOL / GO	0 μM	12.5 μM	50 μM	200 μM
0 ng/ml	✓	✓	✓	✓
0.73 ng/ml	✓	✓		
2.91 ng/ml	✓		✓	
11.7 ng/ml	✓			✓

3.7.1   Cell Viability by Alamar Blue

After treatment for 72 hours, Alamar blue solution (10% v/v) was prepared in complete medium. 100 μl of the solution was added to each well and incubated at 37 °C with 5% CO_2 for 4 hours. As a negative control group, medium without cells was used. The absorption is investigated by micro plate reader (BIO-RAD Mark, Microplate Reader). Percentage of Alamar blue reduction was determined by using the Equation 3.2 [64].

$$\%Reduced = \frac{(\epsilon_{OX}).\lambda_2.A\lambda_1 - (\epsilon_{OX}).\lambda_1.A\lambda_2}{(\epsilon_{red}).\lambda_1.A'\lambda_2 - (\epsilon_{red}).\lambda_1.A'\lambda_2} \times 100 \qquad (3.2)$$

Where,

ϵ_{OX} = molar molar extinction coefficient of alamarBlue oxidized form

ϵ_{red} = molar extinction coefficient of alamarBlue reduced form

A = absorbance of test wells at 570 and 595 nm

A' = absorbance of negative control well at 570 and 595 nm

λ_1 = 570 nm

λ_2 = 595 nm

3.7.2 Cell staining

Solutions of Propidium iodite (PI, sigma) and acridine orange (AO, sigma) was prepared separately in ethanol with concentrations of 3 and 5 mg/ml respectively. To prepare staining solution, 2.5 μl of both solutions were added to 1 ml PBS. Each well was washed two times with PBS. Then 100 μl of the staining solution was added to each well. After 45 seconds, cells washed two times with PBS and the picture was taken by fluorescence microscope immediately [65].

4. RESULTS

4.1 Characterization of Conjugation of ZOL-GO

In this chapter, the conjugation of ZOL and GO was confirmed by using UV-vis spectroscopy, FTIR and AFM. Drug loading and release was analyzed by UV-vis spectroscopy. Finally, the interaction of ZOL-GO with MCF-7 and MSCs was investigated.

4.1.1 UV Analysis

UV-vis spectroscopy is used to characterize the conjugation of ZOL and GO. Figure 4.1 shows UV-vis spectrum of ZOL, GO and ZOL-GO. ZOL and GO peaks are at 209 and 230 nm, respectively. The peaks observed in the UV-vis spectroscopy of ZOL-GO are evidence of stacking of ZOL onto GO. In the UV-vis spectrum of ZOL-GO, the peak which is related to ZOL has a shift from 209 nm to 198 nm.
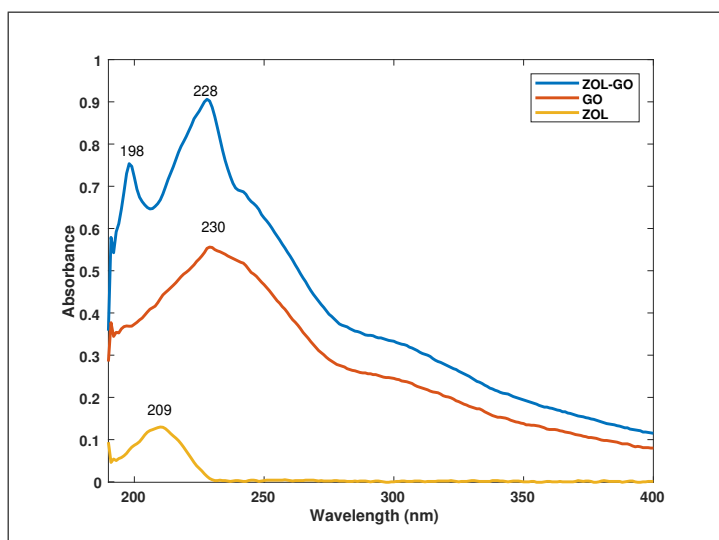

Figure 4.1 UV-vis spectra of ZOL, GO and ZOL-GO in aqueous solution.

4.1.2 FTIR Analysis

The FTIR spectra of ZOL, GO and ZOL-GO are shown Figure 4.3. As it was not possible to have FTIR spectrum of ZOL, the ZOL spectra from Khajuria et al. [66] was taken as reference for ZOL (Figure 4.2).

In the GO spectrum, the band at 3447 cm^{-1} and 3042 cm^{-1} characterizes -OH stretching vibration [67]. As drying GO solution for FTIR experiment might brough back garaphite, the band at 1560 cm^{-1} could be related to skeletal vibration from un-oxidized graphitic domain [68]. The band at 1269 cm^{-1} characterizes C-OH stretching vibration and the band at 901 cm^{-1} ascribes epoxy groups in the GO structure [67]. In the ZOL-GO spectrum, the band at 3480 cm^{-1} and 3049 cm^{-1} characterizes OH group and the band at 1544 cm^{-1} attributes to vibration of CH=CH group in imidazole ring. The band at 1485 cm^{-1} corresponds to stretching vibration of C-H bonds in imidazole ring and the band at 960 cm^{-1} corresponds to stretching vibration of C-C bonds.

The peaks related to hydrogen bonding of ZOL and GO which were respectively 3440 cm^{-1} and 3447 cm^{-1} shifted to 3480 cm^{-1} in the ZOL-GO spectrum. The reason of this shift might be hydrogen interactions between ZOL and GO [69].
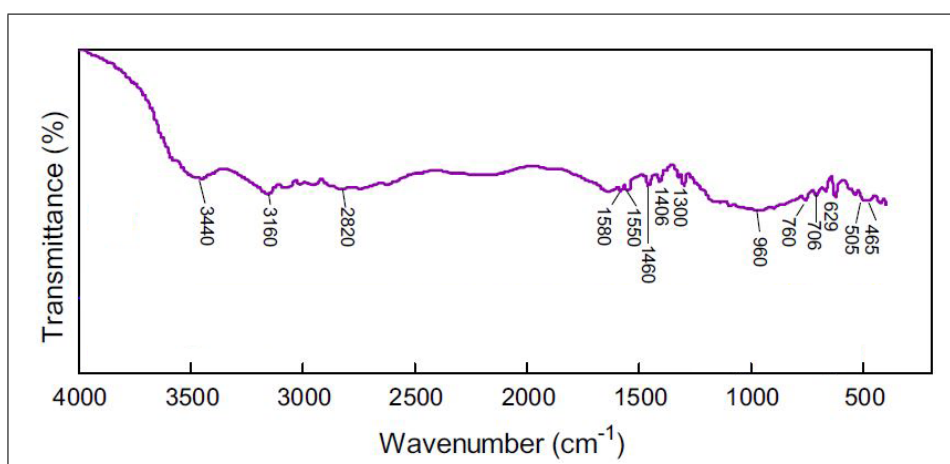
Figure 4.2 FTIR spectra for ZOL [66].

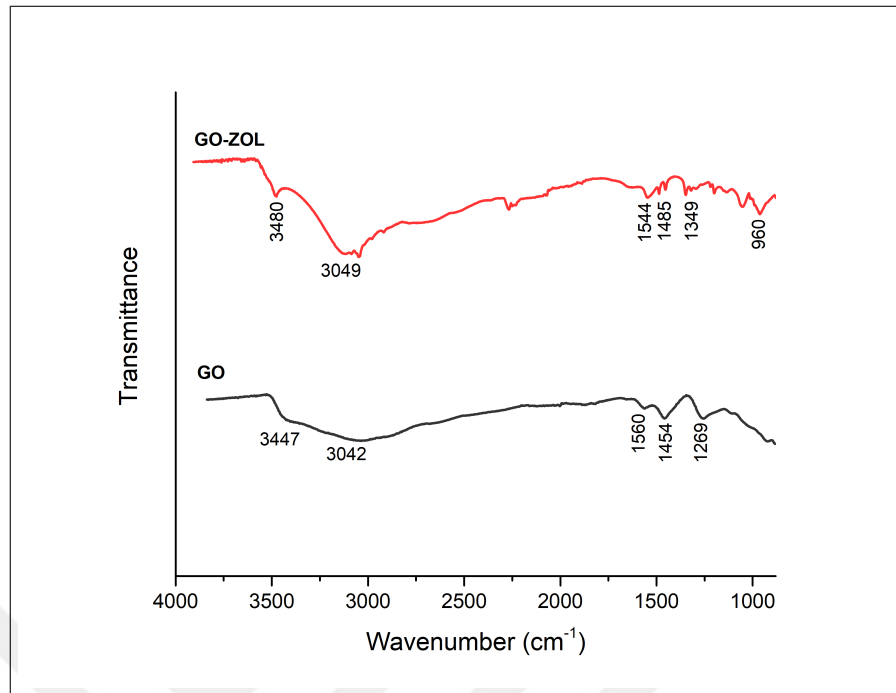**Figure 4.3** FTIR spectra for ZOL-GO.

4.1.3 AFM Analysis

AFM tapping mode was used to characterize GO morphology before and after loading ZOL. As it is shown in Figure 4.4 pure GO shows smoother surface than GO loaded with ZOL. As the samples were washed three times with distilled water, the immobilized particles on GO surface might be ZOL.
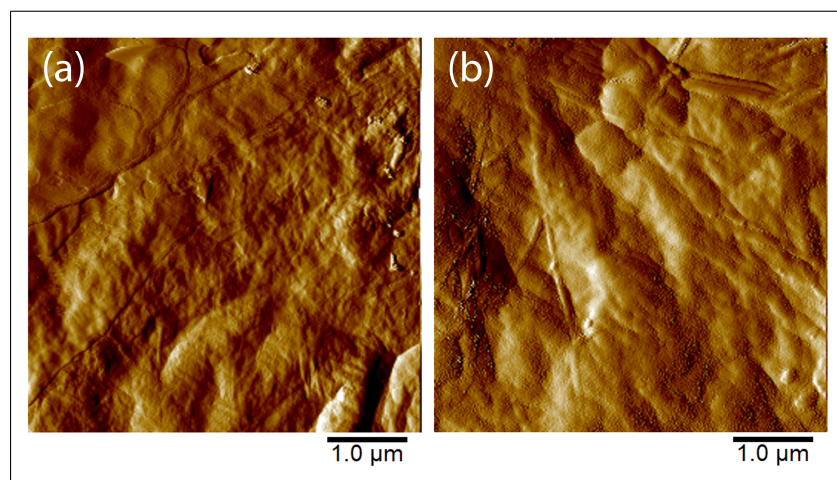
Figure 4.4 AFM image of GO (a) and ZOL-GO (b).

4.2 Drug Loading

Figure 4.5 shows drug loading capacity of ZOL on GO nonoparticles. ZOL to GO ratio of 1:0.2 in the term of mg/ml showed the optimum loading capacity. This proportion have been used after for the other studies such as drug release and cell culture studies.
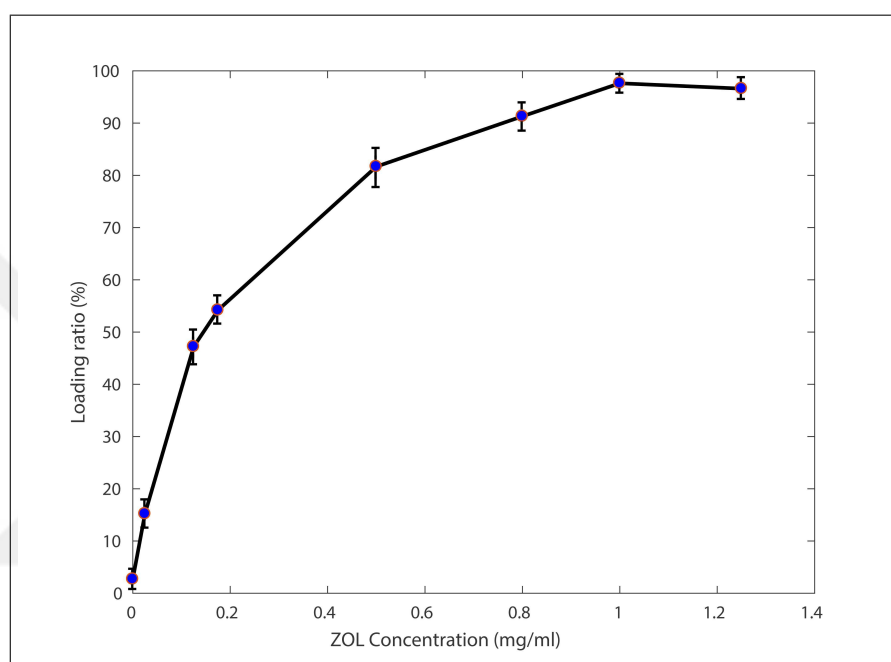
Figure 4.5 Percentage of drug loading on GO.

4.3 Drug Release

The release of ZOL from ZOL-GO complex in PBS at $37 \pm 0.2\,°C$ is shown in Figure 4.6. About 50% of the ZOL was released from ZOL-GO in the first 24 hours and after 50 hours, about 75% of ZOL was detached from ZOL-GO complex.
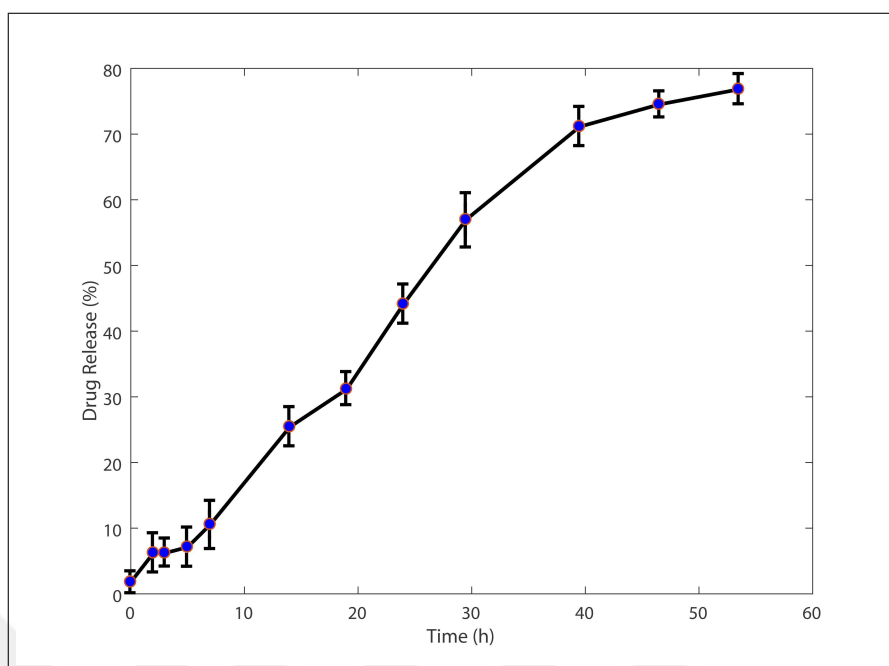
Figure 4.6 In vitro release of ZOL from GO.

4.4 Cell Culture Studies

4.4.1 Cell Viability by Using Alamar Blue

As mentioned before, MCF-7 human breast cancer cells and MSCs were used in order to investigate the effect of different concentrations of ZOL, ZOL-GO and GO on the cells. Alamar blue cell viability assay was used to measure the cytotoxicity of the experimental groups on MCF-7 and MSCs. Top view of an Alamar blue assay for MCF-7 cells is shown in Figure 4.7 . Figure 4.8 and Figure 4.9 show the result of Alamar blue assay for MCF-7 cells and MSCs after 72 hours of treatment with free ZOL, ZOL-GO and GO. According to Figure 4.8 (a), decrease in the reduction of Alamar blue was observed in MCF-7 cells after treatment with ZOL and ZOL-GO which means that treatment with both groups decrease MCF-7 cell viability. In concentrations of 12.5 and 50 μM (in the term of ZOL concentration), we observe lower cell viability after treatment with ZOL-GO compared with treatment with free ZOL. Figure 4.8 (b) shows the result of Alamar blue reduction for MSCs after treatment with mentioned groups. As it is shown in Figure 4.8 (b), MSCs treatment with ZOL and ZOL-GO also result

in decrease in the cell viability. In concentrations of 50 and 200 μM (in the term of ZOL concentration), treatment with ZOL-GO shows lower cell viability compared with the treatment with free ZOL. Figure 4.9 shows a concentration-dependent decrease in cell viability in both MCF-7 cells and MSCs after treatment with ZOL and ZOL-GO. Treatment of both MCF-7 cells and MSCs with GO did not show any significant difference in cell viability compared with control.
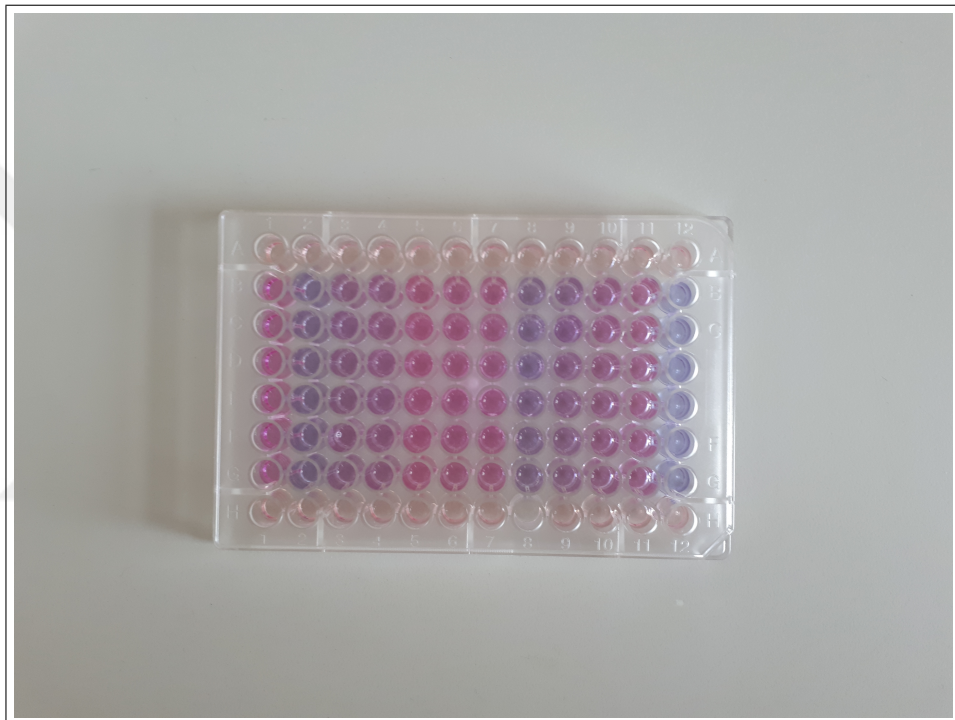
Figure 4.7 Top view of an Alamar blue assay for MCF-7 cells.
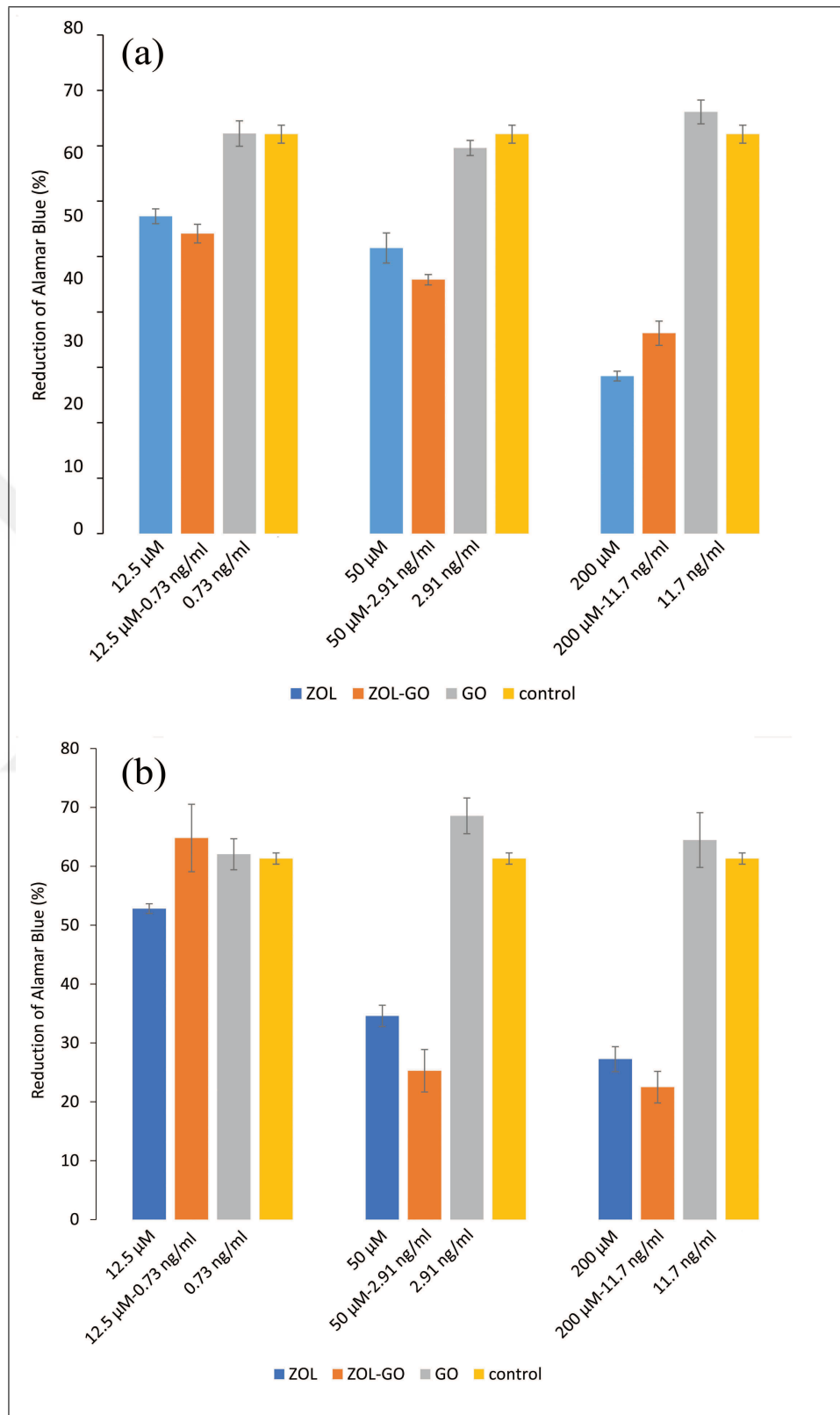
Figure 4.8 Alamar blue assay result at the third day for MCF-7 cells (a) and MSCs (b). Results represent mean ± standard error range.
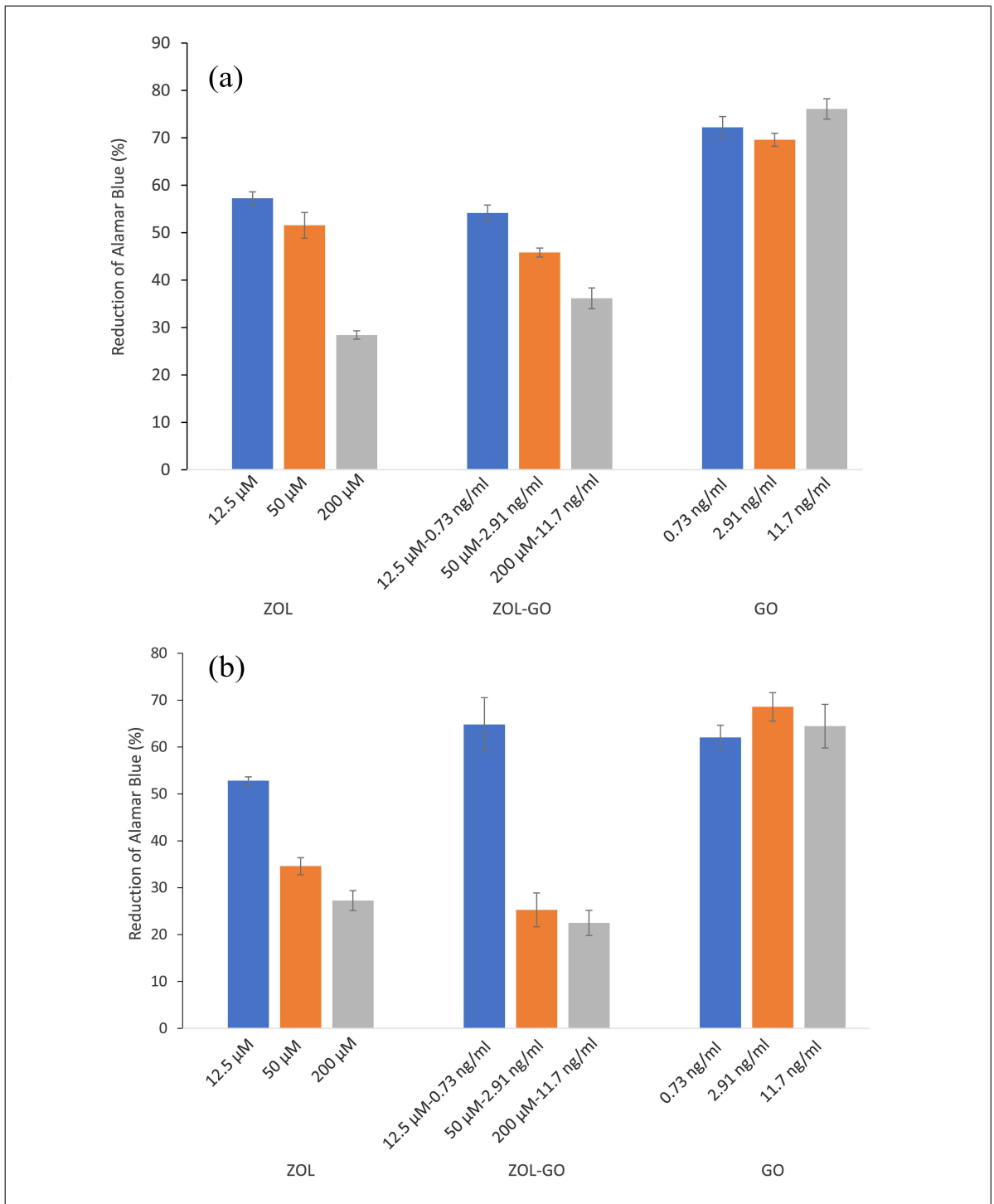
Figure 4.9 Alamar blue assay result at the third day for MCF-7 cells (a) and MSCs (b). Results represent mean ± standard error range.

4.4.2 Cell Staining

In addition to Alamar blue assay, cell staining also confirm the cell culture studies. Figure 4.10 shows the result of staining MCF-7 cells with Propidium Iodide (PI) and Acridine Orange (AO). It was observed that, after treatment with ZOL-GO, the cell viability is lower compared with the treatment of the cells with pure ZOL.

Figure 4.11 shows the result of MSCs staining with AO and PI. The results confirm the cytotoxic effect of ZOL on MSCs.
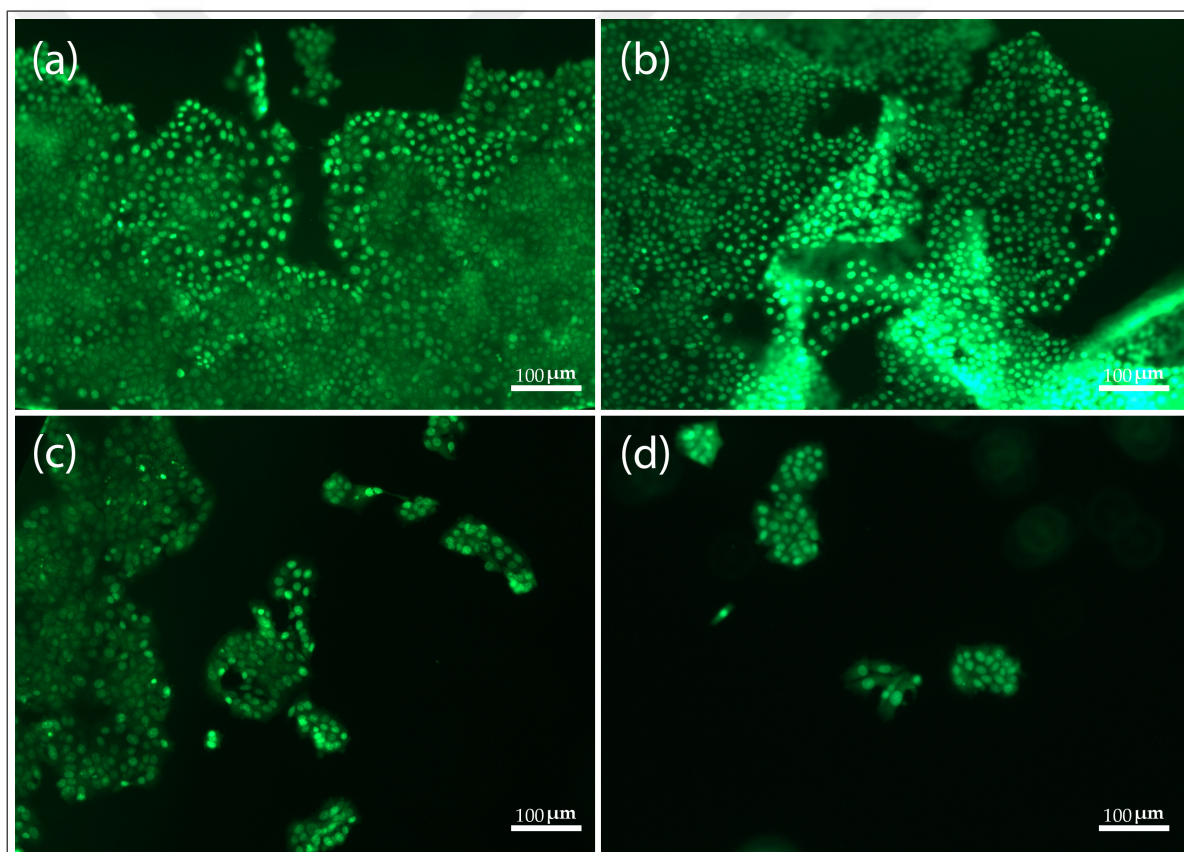
Figure 4.10 MCF-7 cells staining by AO and PI. Untreated (a) treated with 2.91 ng/ml of GO (b), with 50 μM of ZOL (c) and with 50 μM-2.91 ng/ml of ZOL-GO (d).
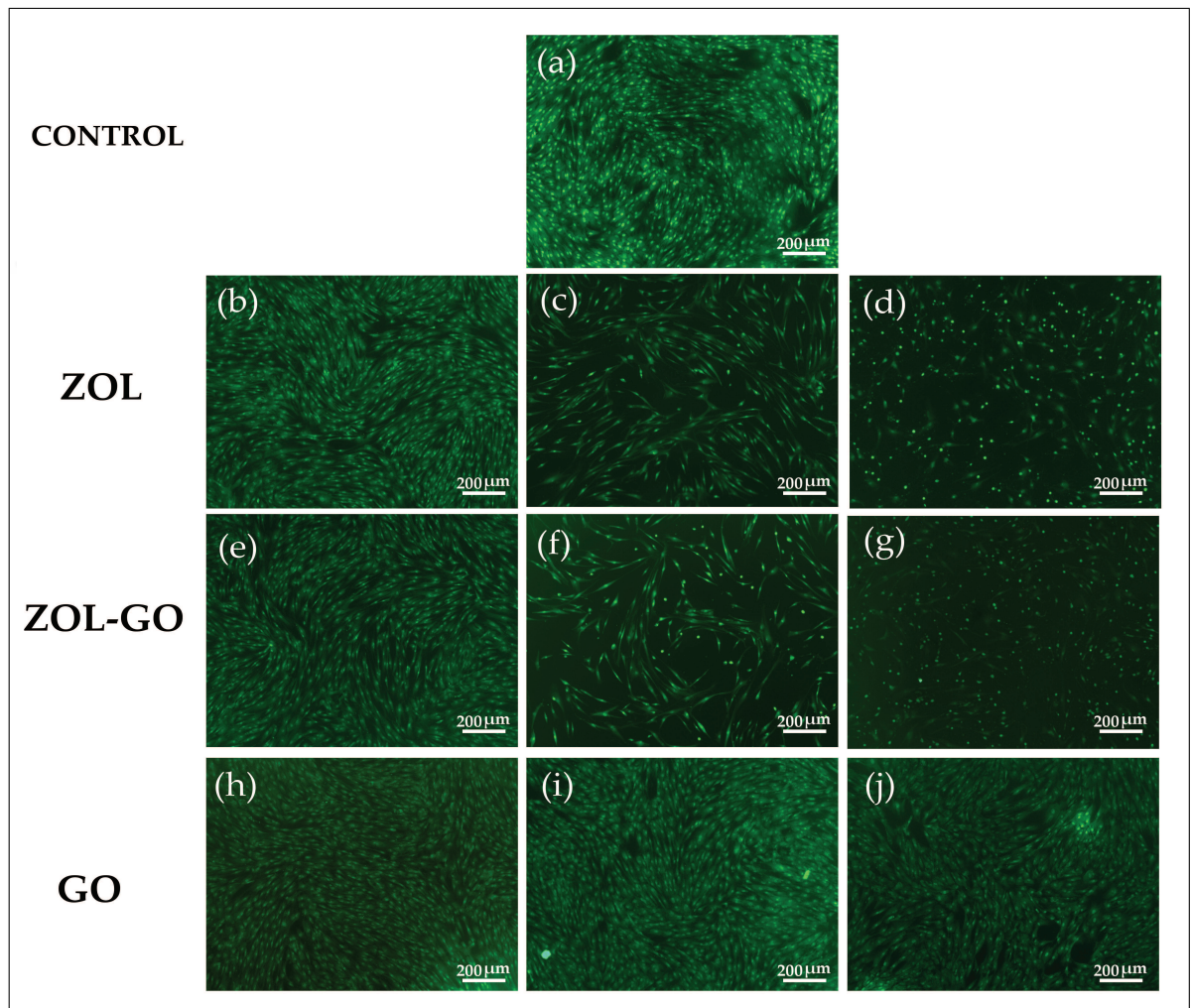
Figure 4.11 MSCs staining by AO and PI. Untreated (a), treated with 12.5 μM of ZOL (b), 50 μM of ZOL(c), 200 μM of ZOL (d), 12.5 μM-0.73 ng/ml of ZOL-GO (e), 50 μM-2.91 ng/ml of ZOL-GO (f), and 200 μM-11.7 ng/ml of ZOL-GO (g), 0.73 ng/ml GO (h), 2.91 ng/ml GO (i) and 11.7 mg/ml GO (j).

5. DISCUSSION

5.1 ZOL-GO Conjugation Characterizations

As it is shown in Figure 4.1, ZOL-GO spectrum has both ZOL and GO peaks but both shifted slightly. The peak in ZOL-GO which is related to GO shifted from 230 nm to 228 nm and the ZOL related peak shifted from 209 nm to 198 nm which might be due to interaction of ZOL and GO [6]. In addition, the FTIR result also confirm the conjugation of ZOL on GO nanoparticles. FTIR spectrum of ZOL and ZOL-GO is shown in Figure 4.3. As mentioned in FTIR result section, we observe some shift in ZOL-GO spectrum which might be due to hydrogen bonding between ZOL and GO . The peaks related to O-H bonds of ZOL and GO were respectively 3440 cm^{-1} and 3447 cm^{-1} which shifted to 3480 cm^{-1} in the ZOL-GO spectrum [6]. furthermore, in the Figure 4.4, GO and ZOL-GO morphology can be observed. GO morphology is smoother compared with ZOL-GO surface and in ZOL-GO surface we observe some particles which might be immobilized ZOL particles on GO surface [6].

5.2 Drug Loading

Drug loading capacity is calculated by using Equation 3.1. Figure 4.5 shows that the optimum loading capacity of GO for ZOL is around 98%. This can be misleading because this percentage merely shows the ratio of loaded ZOL mass to GO mass. It means that even 100% drug loading capacity doesn't mean that all the drug is loaded to drug carrier. Zhang et al. [7] observed more than 400% loading capacity of NGO for DOX. The reason that we observe lower drug capacity might be because DOX has more aromatic rings and as a result, stronger $\pi - \pi$ stacking interactions. In addition, NGO particles has more surface area than GO and this increases degree of DOX loading on GO.

5.3   Drug Release

As it can be observed from drug release profile in Figure 4.6, after 24 hours about 50% of drug is released from the drug complex. Yang et al. [6] used GO as a drug carrier for DOX. This study states that DOX and GO interact via $\pi - \pi$ stacking and hydrophobic interactions and their observations are in good agreement with the drug release results of this work where the conjugation of drug and drug carrier is same as Yang et al. [6] work.

5.4   Cell Studies

As it is shown in Figure 4.9, both treatment with ZOL and ZOL-GO show dose-dependent reduction MCF-7 cell viability. In addition, Figure 4.8 shows that, for 12.5 μM and 50 μM of ZOL, a lower MCF-7 cell viability was observed after treatment with ZOL-GO compared to the treatment with free ZOL. Figure 4.10 shows that cell staining confirmed the results from Alamar blue. GO did not show any significant cytotoxicity on MCF-7 cells. Wu et al. [11] used GO as a drug carrier for ADR which is another type of bisphosphonate. They also observed lower cell viability in the same cancer cell line after treatment with ADR-GO compared to free ADR. Therefore, GO nanoparticle might be a good candidate for loading bisphosphonates.

MSCs studies results are also shown in Figure 4.8 and Figure 4.9. According to the results, treatment of MSCs with ZOL and ZOL-GO show dose-dependent decrease in cell viability. Conjugation of GO to ZOL, did not decrease the cytotoxicity of ZOL on MSCs and we observe even higher cytotoxicity of ZOL-GO in the concentrations of 50 μM and 200 μM .Treatment with different concentration of free GO did not show significant decrease in cell viability. Ebert et al. [12] also observed that ZOL inhibits MSCs proliferation in vitro. The reason is that ZOL inhibits protein farnesylation and geranylgeranylation which is also the reason for osteoclast apoptosis caused by ZOL.

6. CONCLUSION AND FUTURE WORK

Based on the results from UV-vis spectroscopy, FTIR and AFM, we could conclude that the anti-cancer drug ZOL conjugated to GO by π-π stacking and hydrogen-bonding interactions. Conjugation of ZOL to GO could provide other benefits such as increasing drug complex volume and prevent fast renal filtration. Slow release of ZOL from ZOL-GO might keep the moderate dose of drug in the body and eliminate the need for applying high doses of the drug and decrease harmful side effects such as osteonecrosis of the jaw.

In addition, according to the cell culture studies, treatment of MCF-7 cancer cells with ZOL-GO drug complex was more effective in doses of 12.5 and 50 μM compared with free ZOL. As it shown in the results section, in the mentioned doses, we observed lower cell viability after 72 hours of treatment with ZOL-GO rather than free ZOL. These results were also confirmed by cell staining. According to the mentioned results, GO could be a good candidate as a drug carrier for anti-cancer drug ZOL. Treatment of MSCs with free ZOL and ZOL-GO decreases the cell viability significantly. So, using GO as a drug carrier for ZOL would not decrease the cytotoxicity of ZOL on MSCs.

In the future, as some tumor cell lines such as MCF-7 cells over-express folate receptor [70], ZOL-GO drug complex could be used in targeted delivery by conjugating it to folic acid (FA). The effect of ZOL-GO drug complex on other cancer cell lines such as MDA-MB-231 could be investigated. In addition, instead of GO, reduced GO (rGO) might be used as a drug carrier for ZOL and results could be compared with the findings of this study.

APPENDIX A. CALIBRATION CURVE

Table A.1 shows the concentration and absorption of samples which used to calculate ZOL calibratio curve (standard line) and Figure A.2 demonstrate UV-vis spectrum for each sample . Figure A.1 shows ZOL calibration curve and the equation of the line.
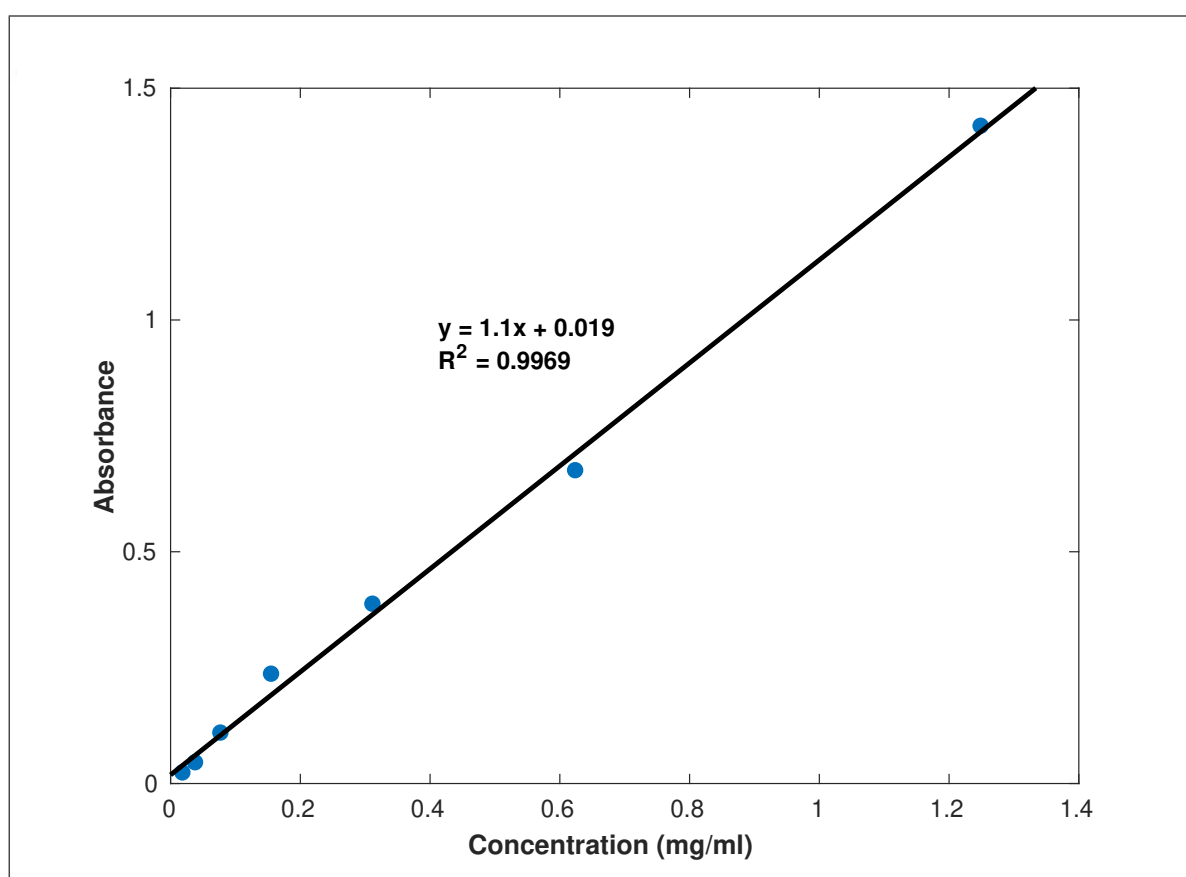
Figure A.1 The calibration curve for ZOL solutions.

Table A.1
List of the samples used for calibration curve.

Sample No.	Concentration (mg/ml)	Molar Concentration (μM)	Absorbance (209 nm)
1	1.25	4308.8	1.417
2	0.625	2154.4	0.674
3	0.3125	1077.2	0.386
4	0.1562	538.6	0.235
5	0.0781	269.3	0.108
6	0.0390	134.6	0.044
7	0.0195	67.3	0.022
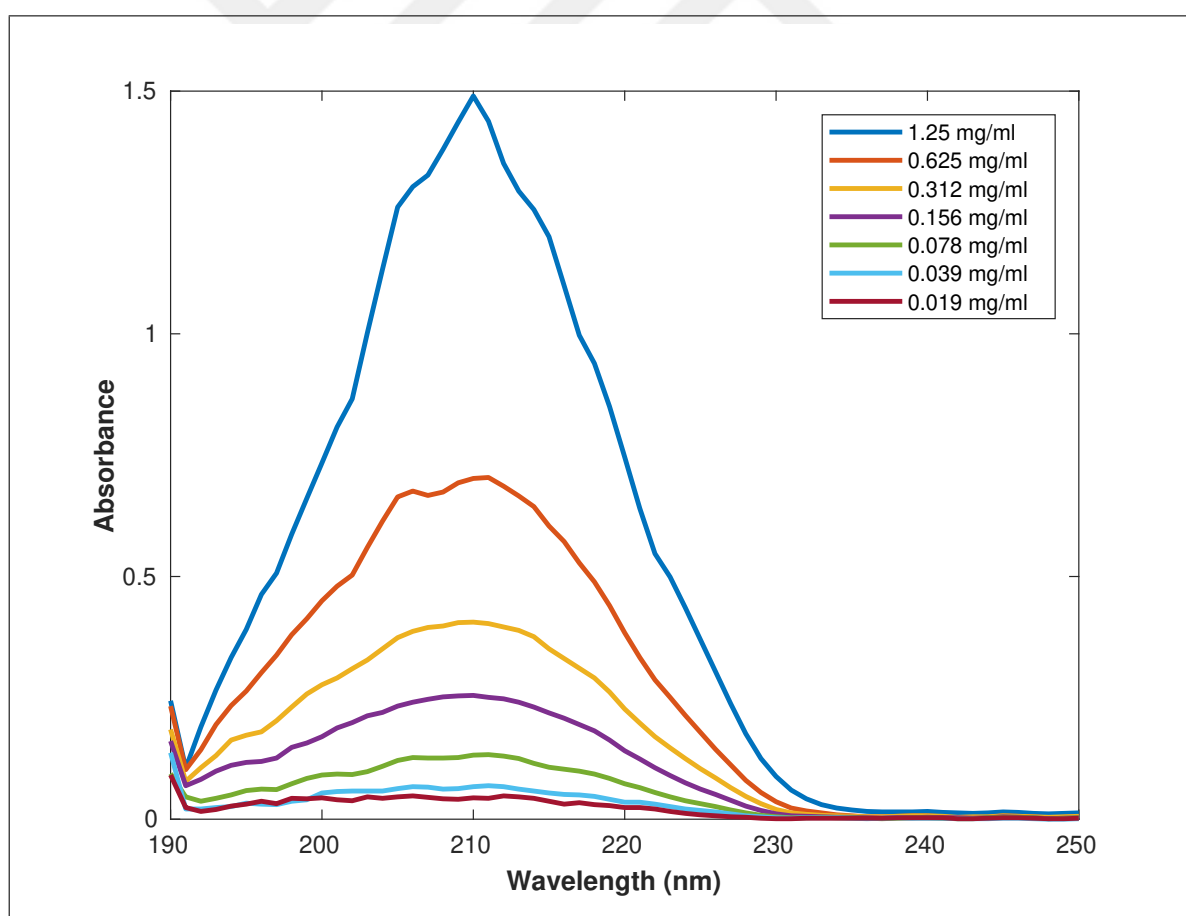
Figure A.2 UV-vis spectra for ZOL solutions.

REFERENCES

1. Nadar, R. A., N. Margiotta, M. Iafisco, J. J. van den Beucken, O. C. Boerman, and S. C. Leeuwenburgh, "Bisphosphonate-functionalized imaging agents, anti-tumor agents and nanocarriers for treatment of bone cancer," *Advanced Healthcare Materials*, 2017.

2. Gnant, M., P. Dubsky, and P. Hadji, "Bisphosphonates: prevention of bone metastases in breast cancer," in *Prevention of Bone Metastases*, pp. 65–91, Springer, 2012.

3. Saad, F., and J.-B. Lattouf, "Bisphosphonates: prevention of bone metastases in prostate cancer," in *Prevention of Bone Metastases*, pp. 109–126, Springer, 2012.

4. Misra, R., S. Acharya, and S. K. Sahoo, "Cancer nanotechnology: application of nanotechnology in cancer therapy," *Drug Discovery Today*, Vol. 15, no. 19-20, pp. 842–850, 2010.

5. Lin, J., "Bisphosphonates: a review of their pharmacokinetic properties," *Bone*, Vol. 18, no. 2, pp. 75–85, 1996.

6. Yang, X., X. Zhang, Z. Liu, Y. Ma, Y. Huang, and Y. Chen, "High-efficiency loading and controlled release of doxorubicin hydrochloride on graphene oxide," *The Journal of Physical Chemistry C*, Vol. 112, no. 45, pp. 17554–17558, 2008.

7. Zhang, L., J. Xia, Q. Zhao, L. Liu, and Z. Zhang, "Functional graphene oxide as a nanocarrier for controlled loading and targeted delivery of mixed anticancer drugs," *Small*, Vol. 6, no. 4, pp. 537–544, 2010.

8. Erez, R., S. Ebner, B. Attali, and D. Shabat, "Chemotherapeutic bone-targeted bisphosphonate prodrugs with hydrolytic mode of activation," *Bioorganic & Medicinal Chemistry Letters*, Vol. 18, no. 2, pp. 816–820, 2008.

9. Torger, B., D. Vehlow, B. Urban, S. Salem, D. Appelhans, and M. Müller, "Cast adhesive polyelectrolyte complex particle films of unmodified or maltose-modified poly (ethyleneimine) and cellulose sulphate: fabrication, film stability and retarded release of zoledronate," *Biointerphases*, Vol. 8, no. 1, p. 25, 2013.

10. Jagdev, S., R. Coleman, C. Shipman, A. Rostami-H, and P. Croucher, "The bisphosphonate, zoledronic acid, induces apoptosis of breast cancer cells: evidence for synergy with paclitaxel," *British Journal of Cancer*, Vol. 84, no. 8, p. 1126, 2001.

11. Wu, J., Y.-s. Wang, X.-y. Yang, Y.-y. Liu, J.-r. Yang, R. Yang, and N. Zhang, "Graphene oxide used as a carrier for adriamycin can reverse drug resistance in breast cancer cells," *Nanotechnology*, Vol. 23, no. 35, p. 355101, 2012.

12. Ebert, R., S. Zeck, R. Krug, J. Meissner-Weigl, D. Schneider, L. Seefried, J. Eulert, and F. Jakob, "Pulse treatment with zoledronic acid causes sustained commitment of bone marrow derived mesenchymal stem cells for osteogenic differentiation," *Bone*, Vol. 44, no. 5, pp. 858–864, 2009.

13. Buenrostro, D., P. L. Mulcrone, P. Owens, and J. A. Sterling, "The bone microenvironment: A fertile soil for tumor growth," *Current Osteoporosis Reports*, Vol. 14, no. 4, pp. 151–158, 2016.

14. Futakuchi, M., K. Fukamachi, and M. Suzui, "Heterogeneity of tumor cells in the bone microenvironment: Mechanisms and therapeutic targets for bone metastasis of prostate or breast cancer," *Advanced Drug Delivery Reviews*, Vol. 99, pp. 206–211, 2016.

15. Sottnik, J. L., J. Dai, H. Zhang, B. Campbell, and E. T. Keller, "Tumor-induced pressure in the bone microenvironment causes osteocytes to promote the growth of prostate cancer bone metastases," *Cancer Research*, Vol. 75, no. 11, pp. 2151–2158, 2015.

16. Giles, A. J., C. M. Reid, J. D. Evans, M. Murgai, Y. Vicioso, S. L. Highfill, M. Kasai, L. Vahdat, C. L. Mackall, D. Lyden, *et al.*, "Activation of hematopoietic stem/progenitor cells promotes immunosuppression within the pre–metastatic niche," *Cancer Research*, Vol. 76, no. 6, pp. 1335–1347, 2016.

17. Criscitiello, C., G. Viale, L. Gelao, A. Esposito, M. De Laurentiis, S. De Placido, M. Santangelo, A. Goldhirsch, and G. Curigliano, "Crosstalk between bone niche and immune system: osteoimmunology signaling as a potential target for cancer treatment," *Cancer Treatment Reviews*, Vol. 41, no. 2, pp. 61–68, 2015.

18. Mundy, G. R., "Metastasis: Metastasis to bone: causes, consequences and therapeutic opportunities," *Nature Reviews Cancer*, Vol. 2, no. 8, p. 584, 2002.

19. Kawatani, M., and H. Osada, "Osteoclast-targeting small molecules for the treatment of neoplastic bone metastases," *Cancer Science*, Vol. 100, no. 11, pp. 1999–2005, 2009.

20. Harris, F., and L. Pierpoint, "Photodynamic therapy based on 5-aminolevulinic acid and its use as an antimicrobial agent," *Medicinal Research Reviews*, Vol. 32, no. 6, pp. 1292–1327, 2012.

21. Santini, D., S. Galluzzo, B. Vincenzi, G. Schiavon, E. Fratto, F. Pantano, and G. Tonini, "New developments of aminobisphosphonates: the double face of janus," *Annals of Oncology*, Vol. 18, no. suppl_6, pp. vi164–vi167, 2007.

22. Santini, D., L. Stumbo, C. Spoto, L. D'Onofrio, F. Pantano, M. Iuliani, A. Zoccoli, G. Ribelli, V. Virzì, B. Vincenzi, *et al.*, "Bisphosphonates as anticancer agents in early breast cancer: preclinical and clinical evidence," *Breast Cancer Research*, Vol. 17, no. 1, p. 121, 2015.

23. Alghamdi, H. S., R. Bosco, S. K. Both, M. Iafisco, S. C. Leeuwenburgh, J. A. Jansen, and J. J. van den Beucken, "Synergistic effects of bisphosphonate and calcium phosphate nanoparticles on peri-implant bone responses in osteoporotic rats," *Biomaterials*, Vol. 35, no. 21, pp. 5482–5490, 2014.

24. Cole, L. E., T. Vargo-Gogola, and R. K. Roeder, "Targeted delivery to bone and mineral deposits using bisphosphonate ligands," *Advanced Drug Delivery Reviews*, Vol. 99, pp. 12–27, 2016.

25. Russell, R. G. G., "Bisphosphonates: the first 40 years," *Bone*, Vol. 49, no. 1, pp. 2–19, 2011.

26. Ebetino, F. H., A.-M. L. Hogan, S. Sun, M. K. Tsoumpra, X. Duan, J. T. Triffitt, A. A. Kwaasi, J. E. Dunford, B. L. Barnett, U. Oppermann, *et al.*, "The relationship between the chemistry and biological activity of the bisphosphonates," *Bone*, Vol. 49, no. 1, pp. 20–33, 2011.

27. Roelofs, A. J., K. Thompson, S. Gordon, and M. J. Rogers, "Molecular mechanisms of action of bisphosphonates: current status," *Clinical Cancer Research*, Vol. 12, no. 20, pp. 6222s–6230s, 2006.

28. Yuasa, T., S. Kimura, E. Ashihara, T. Habuchi, and T. Maekawa, "Zoledronic acid-a multiplicity of anti-cancer action," *Current Medicinal Chemistry*, Vol. 14, no. 20, pp. 2126–2135, 2007.

29. Guenther, A., S. Gordon, M. Tiemann, R. Burger, F. Bakker, J. R. Green, W. Baum, A. J. Roelofs, M. J. Rogers, and M. Gramatzki, "The bisphosphonate zoledronic acid has antimyeloma activity in vivo by inhibition of protein prenylation," *International Journal of Cancer*, Vol. 126, no. 1, pp. 239–246, 2010.

30. Lewiecki, E. M., "Safety of long-term bisphosphonate therapy for the management of osteoporosis," *Drugs*, Vol. 71, no. 6, pp. 791–814, 2011.

31. De Rosales, R. T. M., C. Finucane, S. Mather, and P. Blower, "Bifunctional bisphosphonate complexes for the diagnosis and therapy of bone metastases," *Chemical Communications*, no. 32, pp. 4847–4849, 2009.

32. Junankar, S., G. Shay, J. Jurczyluk, N. Ali, J. Down, N. Pocock, A. Parker, A. Nguyen, S. Sun, B. Kashemirov, *et al.*, "Real-time intravital imaging establishes tumor-associated macrophages as the extraskeletal target of bisphosphonate action in cancer," *Cancer Discovery*, Vol. 5, no. 1, pp. 35–42, 2015.

33. Henneman, Z. J., G. H. Nancollas, F. H. Ebetino, R. G. G. Russell, and R. J. Phipps, "Bisphosphonate binding affinity as assessed by inhibition of carbonated apatite dissolution in vitro," *Journal of Biomedical Materials Research Part A*, Vol. 85, no. 4, pp. 993–1000, 2008.

34. Xie, Y., T. S. H. Perera, F. Li, Y. Han, and M. Yin, "Quantitative detection method of hydroxyapatite nanoparticles based on eu3+ fluorescent labeling in vitro and in vivo," *ACS Applied Materials & Interfaces*, Vol. 7, no. 43, pp. 23819–23823, 2015.

35. Iafisco, M., B. Palazzo, G. Falini, M. Di Foggia, S. Bonora, S. Nicolis, L. Casella, and N. Roveri, "Adsorption and conformational change of myoglobin on biomimetic hydroxyapatite nanocrystals functionalized with alendronate," *Langmuir*, Vol. 24, no. 9, pp. 4924–4930, 2008.

36. Russell, R., N. Watts, F. Ebetino, and M. Rogers, "Mechanisms of action of bisphosphonates: similarities and differences and their potential influence on clinical efficacy," *Osteoporosis International*, Vol. 19, no. 6, pp. 733–759, 2008.

37. Clézardin, P., F. H. Ebetino, and P. G. Fournier, "Bisphosphonates and cancer-induced bone disease: beyond their antiresorptive activity," *Cancer Research*, Vol. 65, no. 12, pp. 4971–4974, 2005.

38. Coxon, F. P., K. Thompson, and M. J. Rogers, "Recent advances in understanding the mechanism of action of bisphosphonates," *Current Opinion in Pharmacology*, Vol. 6, no. 3, pp. 307–312, 2006.

39. Caraglia, M., D. Santini, M. Marra, B. Vincenzi, G. Tonini, and A. Budillon, "Emerging anti-cancer molecular mechanisms of aminobisphosphonates," *Endocrine-Related Cancer*, Vol. 13, no. 1, pp. 7–26, 2006.

40. Van Acker, H. H., S. Anguille, Y. Willemen, E. L. Smits, and V. F. Van Tendeloo, "Bisphosphonates for cancer treatment: mechanisms of action and lessons from clinical trials," *Pharmacology & Therapeutics*, Vol. 158, pp. 24–40, 2016.

41. Fragni, M., S. Bonini, P. Bettinsoli, S. Bodei, D. Generali, A. Bottini, P. Spano, M. Memo, and S. Sigala, "The mir-21/pten/akt signaling pathway is involved in the anti-tumoral effects of zoledronic acid in human breast cancer cell lines," *Naunyn-Schmiedeberg's Archives of Pharmacology*, Vol. 389, no. 5, pp. 529–538, 2016.

42. Nakazawa, T., M. Nakamura, R. Matsuda, F. Nishimura, Y. S. Park, Y. Motoyama, Y. Hironaka, I. Nakagawa, H. Yokota, S. Yamada, *et al.*, "Antitumor effects of minodronate, a third-generation nitrogen-containing bisphosphonate, in synergy with $\gamma\delta$t cells in human glioblastoma in vitro and in vivo," *Journal of Neuro-Oncology*, Vol. 129, no. 2, pp. 231–241, 2016.

43. Nelson, A. R., B. Fingleton, M. L. Rothenberg, and L. M. Matrisian, "Matrix metalloproteinases: biologic activity and clinical implications," *Journal of Clinical Oncology*, Vol. 18, no. 5, pp. 1135–1135, 2000.

44. Derenne, S., M. Amiot, S. Barillé, M. Collette, N. Robillard, P. Berthaud, J.-L. Harousseau, and R. Bataille, "Zoledronate is a potent inhibitor of myeloma cell growth and secretion of il-6 and mmp-1 by the tumoral environment," *Journal of Bone and Mineral Research*, Vol. 14, no. 12, pp. 2048–2056, 1999.

45. Boissier, S., M. Ferreras, O. Peyruchaud, S. Magnetto, F. H. Ebetino, M. Colombel, P. Delmas, J.-M. Delaissé, and P. Clézardin, "Bisphosphonates inhibit breast and prostate carcinoma cell invasion, an early event in the formation of bone metastases," *Cancer Research*, Vol. 60, no. 11, pp. 2949–2954, 2000.

46. Scavelli, C., G. Di Pietro, T. Cirulli, M. Coluccia, A. Boccarelli, T. Giannini, G. Mangialardi, R. Bertieri, A. M. L. Coluccia, D. Ribatti, *et al.*, "Zoledronic acid affects over-angiogenic phenotype of endothelial cells in patients with multiple myeloma," *Molecular Cancer Therapeutics*, Vol. 6, no. 12, pp. 3256–3262, 2007.

47. Hiraga, T., P. J. Williams, A. Ueda, D. Tamura, and T. Yoneda, "Zoledronic acid inhibits visceral metastases in the 4t1/luc mouse breast cancer model," *Clinical Cancer Research*, Vol. 10, no. 13, pp. 4559–4567, 2004.

48. Yamagishi, S.-i., R. Abe, Y. Inagaki, K. Nakamura, H. Sugawara, D. Inokuma, H. Nakamura, T. Shimizu, M. Takeuchi, A. Yoshimura, *et al.*, "Minodronate, a newly developed nitrogen-containing bisphosphonate, suppresses melanoma growth and improves survival in nude mice by blocking vascular endothelial growth factor signaling," *The American Journal of Pathology*, Vol. 165, no. 6, pp. 1865–1874, 2004.

49. Giraudo, E., M. Inoue, and D. Hanahan, "An amino-bisphosphonate targets mmp-9–expressing macrophages and angiogenesis to impair cervical carcinogenesis," *The Journal of Clinical Investigation*, Vol. 114, no. 5, pp. 623–633, 2004.

50. Migianu, E., I. Mallard, N. Bouchemal, and M. Lecouvey, "One-pot synthesis of 1-hydroxymethylene-1, 1-bisphosphonate partial esters," *Tetrahedron Letters*, Vol. 45, no. 23, pp. 4511–4513, 2004.

51. Gittens, S. A., G. Bansal, R. F. Zernicke, and H. Uludağ, "Designing proteins for bone targeting," *Advanced Drug Delivery Reviews*, Vol. 57, no. 7, pp. 1011–1036, 2005.

52. Khosla, S., D. Burr, J. Cauley, D. W. Dempster, P. R. Ebeling, D. Felsenberg, R. F. Gagel, V. Gilsanz, T. Guise, S. Koka, *et al.*, "Bisphosphonate-associated osteonecrosis of the jaw: report of a task force of the american society for bone and mineral research," *Journal of Bone and Mineral Research*, Vol. 22, no. 10, pp. 1479–1491, 2007.

53. Filleul, O., E. Crompot, and S. Saussez, "Bisphosphonate-induced osteonecrosis of the jaw: a review of 2,400 patient cases," *Journal of Cancer Research and Clinical Oncology*, Vol. 136, no. 8, pp. 1117–1124, 2010.

54. Saad, F., J. Brown, C. Van Poznak, T. Ibrahim, S. Stemmer, A. Stopeck, I. Diel, S. Takahashi, N. Shore, D. Henry, *et al.*, "Incidence, risk factors, and outcomes of osteonecrosis of the jaw: integrated analysis from three blinded active-controlled phase iii trials in cancer patients with bone metastases," *Annals of Oncology*, Vol. 23, no. 5, pp. 1341–1347, 2011.

55. Lee, S.-H., R.-C. Chan, S.-S. Chang, Y.-L. Tan, K.-H. Chang, M. C. Lee, H.-E. Chang, and C.-C. Lee, "Use of bisphosphonates and the risk of osteonecrosis among cancer patients: a systemic review and meta-analysis of the observational studies," *Supportive Care in Cancer*, Vol. 22, no. 2, pp. 553–560, 2014.

56. Duncan, R., and M. J. Vicent, "Polymer therapeutics-prospects for 21st century: the end of the beginning," *Advanced Drug Delivery Reviews*, Vol. 65, no. 1, pp. 60–70, 2013.

57. Marra, M., G. Salzano, C. Leonetti, P. Tassone, M. Scarsella, S. Zappavigna, T. Calimeri, R. Franco, G. Liguori, G. Cigliana, *et al.*, "Nanotechnologies to use bisphosphonates as potent anticancer agents: the effects of zoledronic acid encapsulated into liposomes," *Nanomedicine: Nanotechnology, Biology and Medicine*, Vol. 7, no. 6, pp. 955–964, 2011.

58. Kohno, N., K. Aogi, H. Minami, S. Nakamura, T. Asaga, Y. Iino, T. Watanabe, C. Goessl, Y. Ohashi, and S. Takashima, "Zoledronic acid significantly reduces skeletal complications compared with placebo in japanese women with bone metastases from breast cancer: a randomized, placebo-controlled trial," *Journal of Clinical Oncology*, Vol. 23, no. 15, pp. 3314–3321, 2005.

59. Low, S. A., and J. Kopeček, "Targeting polymer therapeutics to bone," *Advanced Drug Delivery Reviews*, Vol. 64, no. 12, pp. 1189–1204, 2012.

60. Marra, M., G. Salzano, C. Leonetti, M. Porru, R. Franco, S. Zappavigna, G. Liguori, G. Botti, P. Chieffi, M. Lamberti, *et al.*, "New self-assembly nanoparticles and stealth liposomes for the delivery of zoledronic acid: a comparative study," *Biotechnology Advances*, Vol. 30, no. 1, pp. 302–309, 2012.

61. Chaudhari, K. R., A. Kumar, V. K. M. Khandelwal, M. Ukawala, A. S. Manjappa, A. K. Mishra, J. Monkkonen, and R. S. R. Murthy, "Bone metastasis targeting: a novel approach to reach bone using zoledronate anchored plga nanoparticle as carrier system loaded with docetaxel," *Journal of Controlled Release*, Vol. 158, no. 3, pp. 470–478, 2012.

62. Liu, Z., J. T. Robinson, X. Sun, and H. Dai, "Pegylated nanographene oxide for delivery of water-insoluble cancer drugs," *Journal of the American Chemical Society*, Vol. 130, no. 33, pp. 10876–10877, 2008.

63. Mohan, V. B., R. Brown, K. Jayaraman, and D. Bhattacharyya, "Characterisation of reduced graphene oxide: Effects of reduction variables on electrical conductivity," *Materials Science and Engineering: B*, Vol. 193, pp. 49–60, 2015.

64. Bonnier, F., M. Keating, T. P. Wrobel, K. Majzner, M. Baranska, A. Garcia-Munoz, A. Blanco, and H. J. Byrne, "Cell viability assessment using the alamar blue assay: a comparison of 2d and 3d cell culture models," *Toxicology in Vitro*, Vol. 29, no. 1, pp. 124–131, 2015.

65. Bank, H. L., "Rapid assessment of islet viability with acridine orange and propidium iodide," *In Vitro Cellular & Developmental Biology*, Vol. 24, no. 4, pp. 266–273, 1988.

66. Khajuria, D. K., R. Razdan, and D. R. Mahapatra, "Development, in vitro and in vivo characterization of zoledronic acid functionalized hydroxyapatite nanoparticle based formulation for treatment of osteoporosis in animal model," *European Journal of Pharmaceutical Sciences*, Vol. 66, pp. 173–183, 2015.

67. Zhang, X., W. Hu, J. Li, L. Tao, and Y. Wei, "A comparative study of cellular uptake and cytotoxicity of multi-walled carbon nanotubes, graphene oxide, and nanodiamond," *Toxicology Research*, Vol. 1, no. 1, pp. 62–68, 2012.

68. Paredes, J., S. Villar-Rodil, A. Martinez-Alonso, and J. Tascon, "Graphene oxide dispersions in organic solvents," *Langmuir*, Vol. 24, no. 19, pp. 10560–10564, 2008.

69. Yang, X., Y. Lu, Y. Ma, Y. Li, F. Du, and Y. Chen, "Noncovalent nanohybrid of ferrocene with single-walled carbon nanotubes and its enhanced electrochemical property," *Chemical Physics Letters*, Vol. 420, no. 4-6, pp. 416–420, 2006.

70. Cao, X., F. Feng, Y. Wang, X. Yang, H. Duan, and Y. Chen, "Folic acid-conjugated graphene oxide as a transporter of chemotherapeutic drug and sirna for reversal of cancer drug resistance," *Journal of Nanoparticle Research*, Vol. 15, no. 10, p. 1965, 2013.